OXFORD

Cerebral Cortex, 2023, **33**, 403–420
https://doi.org/10.1093/cercor/bhac074
Advance access publication date 7 March 2022
Original Article

Multidimensional inhibitory signatures of sentential negation in behavioral variant frontotemporal dementia

Mariano N. Díaz-Rivera[1,2], Agustina Birba[1,3], Sol Fittipaldi[1,3], Débora Mola[4], Yurena Morera[5], Manuel de Vega[5], Sebastian Moguilner[6,7], Patricia Lillo[8,9,10], Andrea Slachevsky[10,11,12,13], Cecilia González Campo[1,3], Agustín Ibáñez[1,3,6,7,*], Adolfo M. García[1,3,6,14,*]

[1]Centro de Neurociencias Cognitivas, Universidad de San Andrés, Vito Dumas 284, Buenos Aires B1644BID, Argentina,
[2]Agencia Nacional de Promoción Científica y Tecnológica (ANPCyT), C1425FQD, Godoy Cruz 2370, Buenos Aires, Argentina,
[3]National Scientific and Technical Research Council (CONICET), C1425FQD, Godoy Cruz 2290, Buenos Aires, Argentina,
[4]Instituto de Investigaciones Psicológicas, CONICET, 5000, Universidad Nacional de Córdoba, Córdoba, Argentina,
[5]Instituto Universitario de Neurociencia (IUNE), Universidad de La Laguna, Campus de Guajara, 38205 La Laguna, Santa Cruz de Tenerife, Spain,
[6]Global Brain Health Institute, University of California, San Francisco, CA94158, US; and Trinity College, Dublin D02DP21, , Ireland,
[7]Latin American Brain Health Institute (BrainLat), Universidad Adolfo Ibáñez, 8320000, Santiago, Chile,
[8]Departamento de Neurología Sur, Facultad de Medicina, Universidad de Chile, 8380000, Santiago, Chile,
[9]Unidad de Neurología, Hospital San José, 8380000, Santiago, Chile,
[10]Geroscience Center for Brain Health and Metabolism (GERO), 7800003, Santiago, Chile,
[11]Neuropsychology and Clinical Neuroscience Laboratory (LANNEC), Physiopathology Department, Neuroscience and East Neuroscience Departments, Faculty of Medicine, Institute of Biomedical Sciences (ICBM), University of Chile, 8380000, Santiago, Chile,
[12]Memory and Neuropsychiatric Clinic (CMYN) Neurology Department, Hospital del Salvador and Faculty of Medicine, University of Chile, 7500000, Santiago, Chile,
[13]Departamento de Medicina, Servicio de Neurología, Clínica Alemana-Universidad del Desarrollo, 7550000, Santiago, Chile,
[14]Departamento de Lingüística y Literatura, Facultad de Humanidades, Universidad de Santiago de Chile, 7550000, Santiago, Chile

*Corresponding authors: Universidad de San Andrés & CONICET, Vito Dumas 284, B1644BID Victoria, Buenos Aires, Argentina. Email: adolfo.garcia@gbhi.org (Adolfo M. García, Ph.D.), agustin.ibanez@gbhi.org (Agustin Ibanez)

Background: Processing of linguistic negation has been associated to inhibitory brain mechanisms. However, no study has tapped this link via multimodal measures in patients with core inhibitory alterations, a critical approach to reveal direct neural correlates and potential disease markers. **Methods:** Here we examined oscillatory, neuroanatomical, and functional connectivity signatures of a recently reported Go/No-go negation task in healthy controls and behavioral variant frontotemporal dementia (bvFTD) patients, typified by primary and generalized inhibitory disruptions. To test for specificity, we also recruited persons with Alzheimer's disease (AD), a disease involving frequent but nonprimary inhibitory deficits. **Results:** In controls, negative sentences in the No-go condition distinctly involved frontocentral delta (2–3 Hz) suppression, a canonical inhibitory marker. In bvFTD patients, this modulation was selectively abolished and significantly correlated with the volume and functional connectivity of regions supporting inhibition (e.g. precentral gyrus, caudate nucleus, and cerebellum). Such canonical delta suppression was preserved in the AD group and associated with widespread anatomo-functional patterns across non-inhibitory regions. **Discussion:** These findings suggest that negation hinges on the *integrity and interaction* of spatiotemporal inhibitory mechanisms. Moreover, our results reveal potential neurocognitive markers of bvFTD, opening a new agenda at the crossing of cognitive neuroscience and behavioral neurology.

Key words: behavioral variant frontotemporal dementia; EEG oscillations; inhibition; multimodal imaging; negation.

Introduction

Negation is a core property of all human languages. In addition to extensive philosophical (Horn 1989) and linguistic (Miestamo 2007) research traditions, accruing neurocognitive evidence highlights its reliance on inhibitory mechanisms (Aravena et al. 2012; Foroni and Semin 2013; Papeo et al. 2016; Beltrán et al. 2018). However, no study has examined this link in brain diseases with differential inhibitory disruptions, let alone integrating neurophysiological, neuroanatomical, and functional connectivity measures. Such an approach would be critical to assess the interplay of inhibitory systems in negation, leading to multidimensional models and potential disease-specific markers. To these ends, we administered a validated Go/No-go negation task to (i) healthy controls (HCs), (ii) patients with behavioral variant frontotemporal dementia (bvFTD, characterized by primary and generalized disinhibitory symptoms), and (iii) persons with Alzheimer's disease (AD, a disease control group with nonprimary inhibitory deficits), capturing online oscillatory traces alongside structural and functional neuroimaging correlates.

Negating is a species-specific capacity supporting critical communicative functions, such as rejection, denial,

Received: November 8, 2021. **Revised:** January 31, 2022. **Accepted:** February 7, 2022

and prohibition (Beltrán et al. 2018, 2019). This process is manifested by multiple linguistic forms, including *no*, *not*, and their counterparts across languages. In particular, since early development, these words are used to signal that particular actions must be interrupted (e.g. *don't touch the knife!*), a tendency that extends into adulthood (e.g. *do not trespass*). Relatedly, their presence in sentences can reduce response speed (Kaup and Zwaan 2003; Kaup et al. 2007) and interfere with manual actions (García-Marco et al. 2019), replicating their effects on daily behavior. Such effects have been attributed to the critical recruitment of inhibitory systems (Foroni and Semin 2013; de Vega et al. 2016; Papeo et al. 2016; Beltrán et al. 2018), responsible for suppressing contextually inappropriate conduct across multiple tasks (Chambers et al. 2009).

This view is supported by neuroscientific research. Electroencephalographic (EEG) studies have targeted frontocentral delta and theta modulations, two critical response inhibition markers (Harmony 2013; Huster et al. 2013), revealing greater power for affirmative than negative sentences in inhibitory contexts—reduced power for negation during inhibition (de Vega et al. 2016; Beltrán et al. 2019). Neuroimaging results consistently link negation with inhibitory regions, including increased activation of inferior frontal and precentral areas (Christensen 2009; Bahlmann et al. 2011), and deactivation of core regions subserving processing of negated action verbs—midfrontal, premotor, primary motor, and posterior cingulate cortices (Tettamanti et al. 2008; Tomasino et al. 2010). This link has been supported by neurostimulation research (Vitale et al. 2022). Thus, insofar as negation suppresses target information (Kaup et al. 2007) while inhibition suppresses motor, cognitive, or affective processes (Phan et al. 2005; Aron and Poldrack 2006), the evidence supports grounded cognition models (Dehaene and Cohen 2007; Pulvermüller 2013; Birba et al. 2017; Pulvermüller 2018) and is fully captured by the "reuse of inhibition for negation" framework, which posits that nonlinguistic inhibitory systems are recycled during negation processing (Beltrán et al. 2021).

However, this research line is undermined by major limitations. First, no study has harnessed strategic neurodegenerative diseases, an approach that has revealed direct correlates of other cognitive domains (Melloni et al. 2015; García-Cordero et al. 2016, 2021; Santamaría-García et al. 2017; Birba et al. 2021). BvFTD represents a relevant condition, as early-stage patients exhibit cardinal (motor and behavioral) inhibitory deficits (Rascovsky et al. 2011), related to critical markers, such as serotonin bioavailability (Hughes et al. 2015). This disease also involves oscillatory abnormalities in the inhibition-sensitive delta band (Chan et al. 2004; Yu et al. 2016; Sami et al. 2018) and other relevant frequencies (Moretti et al. 2016; Ibáñez 2018), as well as anatomofunctional disruptions along inhibitory regions—e.g. precentral, middle and inferior frontal, inferior parietal, and posterior cingulate areas (Lagarde et al. 2013; Hughes et al. 2015; Scheltens et al. 2018; Matías-Guiu et al. 2019). In particular, designs including Alzheimer's disease (AD) patients can reveal whether the mechanisms disrupted in bvFTD are *distinctly* implicated in negation. Inhibitory deficits in AD are not primary diagnostic symptoms; they are typically milder than in bvFTD (Kramer et al. 2003; Stopford et al. 2012) and associated to anteroposterior disruptions (Collette et al. 2002). Importantly, this transdiagnostic approach becomes maximally informative when complemented with multidimensional neural measures (Melloni et al. 2015; Santamaría-García et al. 2017). Yet, negation research has favored individual neuroscientific tools, limiting its theoretical import (for informing multidimensional accounts) and translational potential (for capturing multimodal disease-differential markers) (Uludağ and Roebroeck 2014; Melloni et al. 2016; Salamone et al. 2021). This study aims to circumvent these limitations with the explicit aim of testing hypotheses couched in the "reuse of inhibition for negation" framework (Beltrán et al. 2021).

Specifically, we examined oscillatory, anatomical, and functional connectivity signatures of sentential negation in bvFTD and AD patients relative to HCs. We employed a validated task that manipulates sentence polarity (negative, affirmative) while eliciting response inhibition (de Vega et al. 2016; Beltrán et al. 2019). We computed two critical EEG indexes: a No-go polarity index and the Go polarity index (subtraction between affirmative and negative sentences during No-go and Go trials, respectively). We tested three hypotheses. First, we predicted that, in HCs, the No-go polarity index would show increased delta and/or theta power (reduced power for negative trials). Second, while we anticipated impaired inhibitory performance across diseases, we hypothesized that oscillatory signatures of the No-go polarity index would be selectively disrupted in bvFTD and associated with anatomofunctional disruptions along precentral, midinferior frontal, and posterior cingulate structures implicated in inhibition. Third, we expected that, for the Go polarity index, oscillatory effects in bvFTD patients would not differ from those of HCs or correlate with anatomofunctional patterns. Finally, we hypothesized that, in AD, oscillatory signatures of the No-go polarity index would be preserved and correlated with disease-specific anteroposterior pattern. With this approach, we seek to inform multidimensional accounts of negation while revealing new disease-differential signatures of neurodegeneration.

Materials and methods

Participants

Sixty-two Spanish-speaking individuals, with normal or corrected-to-normal vision, were recruited from two international clinics, in line with recommendations for similar multicentric protocols (Sedeno et al. 2017; Moguilner et al. 2018; Bachli et al. 2020; Salamone et al. 2021). The sample was comprised of 14 bvFTD

Table 1. Demographic and neuropsychological information.

	Healthy controls N = 30	bvFTD patients N = 14	AD patients N = 18	Statistics (all groups)	Pairwise comparisons		
					Groups	Estimate	*P*-value
Demographic data							
Sex (F:M)	18:12	5:9	9:9	—	bvFTD-HCs	1.38	0.23[a]
					AD-HCs	0.14	0.70[a]
Years of age	72.05 (6.65)	68.20 (9.43)	73.30 (4.72)	$F = 1.28$	bvFTD-HCs	−2.77	0.47[c]
				$P = 0.28$[b]	AD-HCs	1.08	0.92[c]
Years of education	13.37 (3.08)	14.95 (5.04)	11.87 (4.39)	$F = 3.89$	bvFTD-HCs	1.59	0.53[c]
				$P = 0.03$[b]	AD-HCs	−2.27	0.18[c]
Neuropsychological data							
MoCA	25.88 (2.26)	21.78 (4.50)	15.11 (6.19)	$F = 36.20$	bvFTD-HCs	−4.09	0.02[c]
				$P < 0.001$[b]	AD-HCs	−10.77	<0.001[c]
Hayling test	7.5 (5.56)	16.28 (12.57)	23.47 (10.62)	$F = 16.22$	bvFTD-HCs	8.78	0.01[c]
				$P < 0.001$[b]	AD-HCs	15.9	<0.001[c]

Data presented as mean (*SD*), except for sex. HCs: healthy controls; bvFTD: behavioral variant frontotemporal dementia; AD: Alzheimer's disease; MoCA: Montreal Cognitive Assessment. [a]*P*-values calculated via chi-squared test (χ^2). [b]*P*-values calculated via independent measures ANOVA. [c]*P*-values calculated via Dunnett's test.

patients, 18 AD patients, and 30 HCs. All but four participants were right-handed (Oldfield 1971). Each patient group was matched with HCs in terms of sex, age, and education (Table 1). Patients were diagnosed by expert neurologists following current clinical criteria for probable bvFTD (Rascovsky et al. 2011) and NINCDS-ADRDA criteria for AD (McKhann et al. 1984, 2011). Diagnoses were supported by an extensive neurological, neuropsychiatric, and neuropsychological examination, as previously reported (Piguet et al. 2011; Baez et al. 2014; Sedeno et al. 2017; García-Cordero et al. 2019).

Each center implemented the Multi-Partner Consortium to Expand Dementia Research in Latin America (ReDLat) standardized diagnostic assessment (Ibanez, Parra, et al. 2021a; Ibanez, Yokoyama, et al. 2021b) to align local sites' procedures. This protocol comprises a brief questionnaire for every participant, including impressions from the neurologist and neuropsychological assessments. Also, all centers used a common training manual for clinical and cognitive evaluation and a quality assurance checklist. These procedures prevent potential biases in participants' assessment and diagnosis across centers.

BvFTD patients were in early/mild stages and exhibited sociobehavioral impairments as defined by caregivers (Neary et al. 1998; Piguet et al. 2011; Ibanez and Manes 2012). Moreover, they presented with predominantly temporo-hippocampal atrophy in both hemispheres (Supplementary Material 1). AD patients showed atrophy across extended bilateral temporomedial areas, including the left hippocampus, the right amygdala, and, to a lesser extent, bilateral frontal and left cerebellar areas (Supplementary Material 1). Cognitive status and semantic inhibition were assessed through the Montreal Cognitive Assessment (MoCA) (Nasreddine et al. 2005) and the Hayling test (Burgess and Shallice 1997), respectively (Table 1). No patient reported a history of other neurological disorders, psychiatric conditions, or substance abuse. HCs were cognitively preserved, were functionally autonomous, and had no background of neuropsychiatric disease or alcohol/drug abuse. Each volunteer signed a written informed consent. The study was performed pursuant to the Declaration of Helsinki and approved by the institutional ethics' committees.

Experimental task

Materials

The experiment involved 166 Spanish sentences from a published version of the same task (de Vega et al. 2016; Beltrán et al. 2019; Liu et al. 2020). These stimuli comprised 83 affirmative sentences and a negative version of each of them ($n = 166$). Each participant responded to half the sentences in the affirmative and the other half in the negative, the polarity of each sentence being counterbalanced across participants (accordingly, all relevant psycholinguistic variables were perfectly matched across conditions). All sentences had an identical structure, beginning with the adverb *Ahora* (now), followed by a polarity marker (*sí* for affirmative sentences, *no* for negative sentences), an action verb in the second person singular of the imperfect future tense (e.g. *cortarás—will cut*), and a direct object (made up of a definite article and a noun) that was coherent with the preceding verb (e.g. *el pan—the bread*)—this example sentence translates roughly into *Now you will/won't cut the bread*. Crucially, the verb was accompanied by a cue that, depending on its color, indicated that the participants should either press a key (Go items) or refrain from doing so (No-go items). To generate a prepotent tendency to respond and thus ensure the taxing of inhibitory mechanisms in the No-go trials, 116 of the trials per subject (70%) featured a Go cue, and the remaining 50 (30%) featured a No-go cue. Half of the Go cues appeared in affirmative sentences and the other half appeared in negative sentences. The same was true for the No-go cues. Therefore, the experiment comprised 58 affirmative Go trials, 58 negative Go trials, 25 affirmative No-go trials, and 25 negative No-go trials. Also, to ensure sustained attention during sentence

reading, a forced-choice yes/no verification question was subsequently presented after 40% of the sentences.

Procedure

Each participant responded to 166 experimental trials, evenly divided across conditions into two blocks. Trials were presented randomly within each block. Each of them began with a fixation point in the center of the screen (500 ms), followed by the whole sentence presented word by word. All words, except the sentence's verb segment, were followed by a 150-ms blank. The first word (*Ahora*) was presented for 200 ms, followed by the sentence polarity marker (*sí/no*) for 300 ms. The verb segment, where the Go/No-go cue was displayed, lasted 600 ms overall, with the following sequence of events: first, the verb appeared for 300 ms; then, the Go/No-go cue (yellow circle for Go, blue circle for No-go) appeared above the verb for 150 ms; finally, upon disappearance of the cue, the verb remained visible for another 150 ms. After the final sequence of the verb, another blank screen was presented for 150 ms, followed by a definite article (e.g. *el*) for 200 ms and then a noun (e.g. *pan*) for 300 ms. A blank screen was then shown for another 300 ms.

Participants were instructed to attentively read each word in the sentence and press a yellow button on the keyboard whenever a yellow cue appeared above the verb (Go trials) and to refrain from pressing the button whenever a blue cue appeared (No-go trials). As previously stated, 40% of the trials were followed by a verification task, which consisted of an initial question mark in the center of the screen (300 ms), followed by the verification sentence (which could match the preceding sentence or not). For these verification items, participants were instructed to press the left arrow if the new sentence matched the preceding one and to press a right arrow if it did not. Prior to the task, for familiarization purposes, participants completed 16 practice trials, the first five corresponding to the Go condition and the remaining seven varying randomly between Go and No-go trials. The practice trials were repeated if so requested. Overall, the experiment lasted roughly 15 minutes. The temporal structure of the task is diagrammed in Fig. 1.

Behavioral data analysis

Overall motor inhibitory performance was inspected by collapsing both affirmative and negative trials for both the No-go and the Go condition. Go trials were analyzed after removing those with RTs below 100 ms (~1.41%). Out of the remaining trials, those below or above 2.5 SDs from the participant's mean (1.7%) were also excluded. Likewise, for commission errors, trials were excluded from analysis if their RT was below 100 ms (~16%) or exceeded 2.5 SDs from the participant's mean (~6.14%). The remaining trials amount did not differ across groups for the Go condition [$F(2, 4617) = 1.94$, $P = 0.14$] or commission errors [$F(2, 166) = 1.16$, $P = 0.31$].

First, to inspect the overall manifestation of inhibitory performance per se, we collapsed all Go trials (affirmative and negative), on the one hand, and all No-go trials (affirmative and negative), on the other, and ran a 3×2 linear mixed effects model, with one between-subject factor (group: HC, bvFTD, AD) and one within-subject factor (condition: Go, No-go). Also, following previous reports of the same paradigm (de Vega et al. 2016; Beltrán et al. 2019; Liu et al. 2019), we performed separate analyses for commission errors (on No-go trials) and omission errors (on Go trials), as well as for reaction times (RTs) in correct Go trials and in commission errors on No-go trials. For each of those analyses, we implemented a 3×2 linear mixed effects model, with one between-subject factor (group: HC, bvFTD, AD) and one within-subject factor (polarity: affirmative, negative). Significant effects were further inspected via Tukey's HSD post-hoc tests. Effect sizes were calculated through partial eta-squared (ηp2) for main and interaction effects, and via Cohen's *d* for pairwise comparisons. Alpha levels were set at $P < 0.05$. All behavioral analyses were performed on *R* (version 3.5.2).

Hd-EEG methods

Data acquisition and preprocessing

Hd-EEG activity was recorded online throughout the task for each participant. Signals were acquired via a BioSemi Active Two 128 Channel System with preamplified sensors and a DC coupling amplifier, at a sampling rate of 1024 Hz. Analog filters were set at 0.03 and 100 Hz. A digital bandpass filter between 0.5 and 50 Hz was applied offline to remove unwanted frequency components. The reference was set to link mastoids for recordings and re-referenced offline to the average of all electrodes. In line with reported procedures (Vilas et al. 2019; Birba et al. 2020; Dottori et al. 2020; García et al. 2020; Cervetto et al. 2021), eye movements or blink artifacts were corrected with independent component analysis (Kim et al. 2012) and with a visual inspection protocol (García-Cordero et al. 2016, 2017; Cervetto et al. 2021). Bad channels were replaced via statistically weighted spherical interpolation (based on all sensors) (Courellis et al. 2016). Epochs were selected from continuous data in a window of −2.5 to 2.5 around the Go/No-go cue. All EEG signal processing steps were implemented on MATLAB software (vR2016a) through the EEGLAB (v14.1.2) toolbox.

Time–frequency analyses

All analyses were run on the Fieldtrip Toolbox (Oostenveld et al. 2011). First, we computed the time–frequency representation (TFR) by convolving four-cycle complex Morlet wavelets with 2 Hz steps for each single-trial epoch to obtain the targeted spectral power (1–40 Hz). As in previous reports of this task (de Vega et al. 2016; Beltrán et al. 2019), the mean of event-related power synchronization across trials was calculated for each condition and subject, with a baseline of 500 ms before the polarity marker (*sí/no*) appeared (−1150, −650 ms).

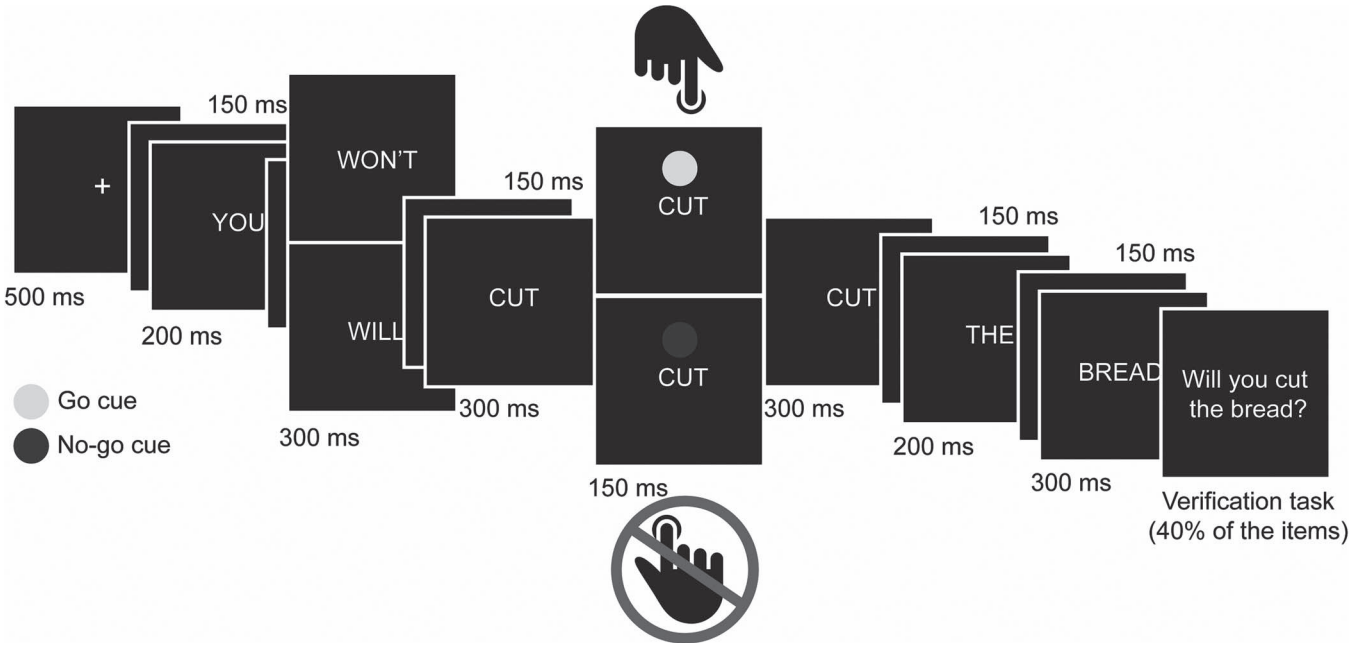

Fig. 1. Temporal structure of the experimental task. Participants first viewed a fixation cross, followed by a word-by-word sentence with the following structure: *Ahora + sí/no + verb + definite article + noun* (e.g. *Ahora sí/no cortarás el pan* [*Now you will/won't cut the bread*]. A cue circle appeared above verb, prompting participants to either press a key (lighter color circle) or refrain from doing so (darker color circle). To ensure sustained attention during sentence reading, a forced-choice yes/no verification question was subsequently presented after 40% of the sentences.

We calculated the power for each trial relative to its respective baseline and then averaged the ensuing values across trials per subject. The single-trial time–frequency representations in each band were averaged separately for each of the four experimental conditions (affirmative No-go; negative No-go; affirmative Go; negative Go).

Within-group analyses

To detect canonical oscillatory signatures of response inhibition, we first collapsed all affirmative and negative trials corresponding to the No-go and Go conditions. Then, we conducted a within-group analysis in HCs comparing power modulations between No-go and Go trials (henceforth, "inhibitory index"). We further performed a one-tailed cluster-based permutation analysis on time–frequency data based on previous research (de Vega et al. 2016; Beltrán et al. 2019). Analyses were performed targeting two canonic inhibitory frequency bands (delta: 2–3 Hz; theta: 4–7 Hz) and an additional band to test for specificity (alpha: 8–12 Hz).

To detect inhibitory oscillatory signatures of negation, we followed the same approach described above. First, we compared power modulations in HCs between affirmative and negative sentences in No-go trials (henceforth, "No-go polarity index"), as in previous reports of the same task (de Vega et al. 2016; Beltrán et al. 2019). To test for specificity, we applied the same procedure on Go trials (henceforth, "Go polarity index"). Analyses were performed in two target frequency bands (delta: 2–3 Hz; theta: 4–7 Hz) assessed in previous reports of this task (de Vega et al. 2016; Beltrán et al. 2019), together with an additional control band (alpha: 8–12 Hz).

Between-group analyses

To examine possible inhibitory disruptions, we compared power modulations of the inhibitory index between HCs and each patient group. To this end, the specific spatiotemporal cluster obtained in HCs was used as a mask for every patient to calculate his or her own inhibitory indexes. Each participant's mean was compared among all three groups via an omnibus permutation test analogous to a one-way analysis of variance using the function "aovperm" from the R package "permuco" (Frossard et al. 2021). Post-hoc comparisons were performed via two-sample pairwise permutation tests with Bonferroni correction. The alpha level was set to 0.05.

In a similar fashion, to examine potential oscillatory inhibitory alterations during negation processing, we compared power modulations between HCs and all patient groups. The specific spatiotemporal cluster underlying the No-go polarity index in HCs was used as a mask in each patient group to calculate his or her own No-go polarity indices. The ensuing results were compared among all three groups via an omnibus permutation test. Post-hoc comparisons were performed via two-sample pairwise permutation tests with Bonferroni correction. The alpha level was set to 0.05. These nonparametric methods are preferred to minimize the impact of possible extreme values, guaranteeing robustness without compromising statistical power (Hayes 1996). The exact same procedure was repeated for Go trials, to reveal whether predicted alterations in the patient groups were specific to the No-go polarity index (i.e. negation-specific modulations during response inhibition).

Neuroimaging methods

Data acquisition

MRI acquisition and preprocessing steps are reported in line with the practical guide from the Organization for Human Brain Mapping (Nichols et al. 2017; Poldrack et al. 2017). We obtained whole-brain T1-weighted anatomical 3D scans from 26 HCs, 12 bvFTD patients, and 12 AD patients—these groups were also matched for sex, age, and education (Supplementary Material 2, Table S2). Additionally, resting-state functional MRI (fMRI) recordings were obtained for all of them, except one bvFTD patient, who did not take part in that session. For this protocol, participants were asked to keep their eyes closed, not to think about anything in particular, and to avoid moving or falling asleep. Structural and resting-state acquisition parameters for each center are reported in Supplementary Material 3.

MRI data preprocessing

For VBM analysis, data were processed using the DARTEL Toolbox following validated procedures (Ashburner and Friston 2000; García-Cordero et al. 2016; Sedeno et al. 2017) via the Statistical Parametric Mapping software (SPM12) (http://www.fil.ion.ucl.ac.uk/spm/software/spm12/). T1-weighted images in native space were first segmented using the default parameters of the SPM12 (bias regularization was set to 0.001 and bias FWHM was set to 60-mm cutoff) into white matter (WM), gray matter (GM), and cerebrospinal fluid (CFS) (these three tissues were used to estimate the total intracranial volume, TIV). DARTEL (create template) module was run later using the GM and WM segmented images—following SPM12 default parameters—to create a template that is generated from the complete dataset (increasing the accuracy of intersubject alignment) (Ashburner and Friston 2000). Next, we used the "Normalise to MNI Space" module from DARTEL Tools to affine register the last template from the previous step into the MNI Space. This transformation was applied to all the individual GM-segmented scans to also be brought into standard space. Subsequently, all images were modulated to correct volume changes by Jacobian determinants and to avoid bias in the intensity of an area due to its expansion during warping. Finally, data were smoothed using a 10-mm full-width-at-half-maximum isotropic Gaussian kernel to accommodate for intersubject differences in anatomy. The size of the kernel was selected based on previous recommendations (Ashburner and Friston 2000; Good et al. 2001; Burton et al. 2004).

Based on previous literature (Jack et al. 1997; La Joie et al. 2012; Ossenkoppele et al. 2015; van Loenhoud et al. 2017), in order to analyze the images of each center together and avoid a resonator effect in our results, the normalized and smoothed DARTEL outputs were transformed to w-score images. W-scores, similar to Z-scores (mean = 0, SD = 1), represent the degree to which the observed GM volume in each voxel is higher or lower (positive or negative W-score) than expected, based on an individuals' global composite score adjusted for specific covariates (age, disease, TIV, and scanner type). W-scores were calculated for the healthy control sample of each acquisition center, dividing subjects' observed and predicted GM volumes (residuals) by their standard deviation, resulting in W-score maps for each subject.

Resting-state fMRI data preprocessing

The first five volumes of each subject's resting-state sequence were discarded to ensure that magnetization achieved a steady state. Then, images were then preprocessed using the Data Processing Assistant for Resting-State fMRI (DPARSF V2.3) (Chao-Gan and Yu-Feng 2010) (http://rfmri.org/DPARSF), an open-access toolbox that generates automatic pipeline for fMRI analysis by calling the SPM 12 and the Resting-State fMRI Data Analysis Toolkit (REST V.1.7). Following previous studies (Salamone et al. 2018; Yoris et al. 2018; Fittipaldi et al. 2020), preprocessing steps included slice-timing correction (using middle slice of each volume as the reference scan), realignment to the first scan of the session to correct head movement (SPM functions), normalization to the MNI space using the echo-planar imaging (EPI) template from SPM (Ashburner and Friston 1999), smoothing using a 8-mm full-width-at-half-maximum isotropic Gaussian kernel (SPM functions), and bandpass filtering (0.01–0.08 Hz). Six motion parameters, CFS, and WM signals were regressed to reduce the effect of motion and physiological artifacts such as cardiac and respiration effects (REST V1.7 toolbox). Motion parameters were estimated during realignment, and CFS and WM masks were derived from the tissue segmentation of each subject's T1 scan in native space with SPM12 (after coregistration of each subject's structural image with the functional image). Participants did not show translation movements greater than 3 mm and/or rotations higher than 3°. Finally, there were no statistically significant differences between groups in the different estimated motion parameters (Supplementary Material 4, Table S3).

Association between oscillatory indices and brain volume

SPM12 was used to perform multiple regression analyses to assess associations between gray matter volume and (i) No-go polarity index and (ii) the Go polarity index. To increase power and data variance, each patient group (bvFTD, AD) was included alongside the HC group, as in previous works (Sollberger et al. 2009; O'Callaghan et al. 2016; Salamone et al. 2021). TIV was added as a covariate of no interest. As this is an exploratory study with a modest sample size, statistical significance was set to $P < 0.001$, uncorrected, with an extent threshold of 30 voxels. These parameters match recommended lower limits for the power levels reached by our study (Woo et al. 2014), circumventing biases of liberal primary thresholds on false positives and achieving good balance between Type-I and Type-II errors (Lieberman and Cunningham 2009), as in previous imaging studies

Table 2. Accuracy and response time measures on overall inhibitory performance.

	Healthy controls $N = 30$	bvFTD patients $n = 14$	AD patients $n = 18$	Statistics (all groups)	Pairwise comparisons		
					Groups	Estimate	*P*-value
Overall error rate	0.07 (0.09)	0.22 (0.31)	0.42 (0.48)	$F = 25.70$	bvFTD-HCs	−1.15	0.02[b]
				$P = 0.001$[a]	AD-HCs	0.35	<0.001[b]
Commission errors	0.05 (0.07)	0.05 (0.1)	0.06 (0.09)	$F = 24.47$	bvFTD-HCs	0.003	1.00[b]
				$P < 0.01$[a]	AD-HCs	0.009	0.99[b]
Omission errors	0.09 (0.10)	0.39 (0.35)	0.78 (0.41)	$F = 24.47$	bvFTD-HCs	−0.30	<0.01[b]
				$P < 0.01$[a]	AD-HCs	0.68	<0.001[b]
Overall response time	0.54 (0.16)	0.62 (0.20)	0.62 (0.20)	$F = 5.91$	bvFTD-HCs	−0.10	0.008[b]
				$P = 0.004$[a]	AD-HCs	0.09	0.03[b]

Data presented as mean (*SD*). HCs: healthy controls; bvFTD: behavioral variant frontotemporal dementia; AD: Alzheimer's disease. [a]*P*-values calculated via independent measures ANOVA. [b]*P*-values calculated via Tukey HSD post-hoc test.

(Donix et al. 2013; Irish et al. 2014; Melloni et al. 2016; Sedeno et al. 2017; de la Fuente et al. 2019; Santamaría-García et al. 2019) and FC (Yu-Feng et al. 2007; Jabbi et al. 2008; Kanske et al. 2016).

Association between oscillatory indices and resting-state fMRI connectivity

We explored associations between resting-state functional connectivity (rs-FC) data and (i) No-go polarity index and (ii) the Go polarity index. First, for each subject, we extracted the mean time course of the BOLD signal in each of the 116 regions of the Automated Anatomical Labelling Atlas (Tzourio-Mazoyer et al. 2002), by averaging the signal in all voxels comprising each region. Second, we constructed a connectivity matrix for each subject indicating the strength of association between all pairs of regions (Pearson's correlation coefficient; DPARSF toolbox). Third, we performed a Fisher z-transformation. Finally, to prevent scanner type effects in our results, we performed a site normalization following published procedures for multicenter-imaging data (Donnelly-Kehoe et al. 2019). The rs-FC data of each subject (patients and HCs) was z-scored based on the mean and *SD* of the corresponding centers' HC group (Donnelly-Kehoe et al. 2019). The resulting rs-FC z-scores between all pairs of regions were used to perform Spearman's correlations with (i) No-go polarity index and (ii) Go polarity index for each tandem of patients and HCs. To consider results as significant, the alpha level was set at $P < 0.001$ (uncorrected). Only positive associations are reported (Fittipaldi et al. 2020; Salamone et al. 2021).

Results

Behavioral results

Behavioral results revealed a higher error rate for bvFTD and AD patients compared to HCs. Commission errors did not differ significantly across groups. Commission errors on No-go trials revealed nonsignificant main and interaction effects. Omission errors on Go trials were significantly greater for bvFTD and AD patients than for HCs. RTs for correct Go trials were slower for bvFTD and AD than HCs. For statistical details, see Table 2 and Supplementary Material 5.

Time–frequency results

Results from healthy controls

In HCs, the inhibitory index yielded a higher theta power increase for No-go trials than Go trials over an occipito-fronto-central cluster ranging from 0 to 620 ms [$T_{(maxsum)} = 4193.56$, $P = 0.02$]. No other band yielded significant effects (all *P*-values > 0.05)—Supplementary Material 6, Fig. S1.

Also, in HCs, the No-go polarity index involved higher delta power (for affirmative than negative sentences) over a frontocentral cluster from cue onset to 469 ms [$T_{(maxsum)} = 2906.24$, $P = 0.01$]—Fig. 2A1. No other band yielded significant effects (all *P*-values > 0.54). The Go polarity index yielded no significant effects in any band (all *P*-values > 0.05).

Comparisons between healthy controls and patient groups

The comparison between HCs and patient groups for the inhibitory index relating to theta modulations yielded a significant main effect of group [$F(2, 59) = 3.02$, $P < 0.05$]. A post-hoc two-sample pairwise permutation test showed that the bvFTD group significantly differed from HCs [$t = 2.51$, $P = 0.03$, $d = 0.87$], there being no significant differences between HCs and AD patients ($t = -.72$, $P > 0.05$, $d = 0.21$).

The comparison between HCs and patient groups yielded a significant main effect of group for the No-go polarity index [$F(2, 59) = 2.83$, $P = 0.004$]. A post-hoc two-sample pairwise permutation test showed that the bvFTD group significantly differed from HCs [$t = 3.069$, $P = 0.006$, $d = 1.11$], there being no significant differences between HCs and AD patients ($t = -2.35$, $P = 0.06$, $d = 0.74$)—Fig. 2A2, left inset. In contrast, the Go polarity index revealed a nonsignificant effect of group [$F(2, 59) = 1.42$, $P = 0.27$]—Fig. 2A2, right inset.

Associations between oscillatory indices and gray matter volume

Associations between oscillatory indices and gray matter volume revealed differential patterns in each patient

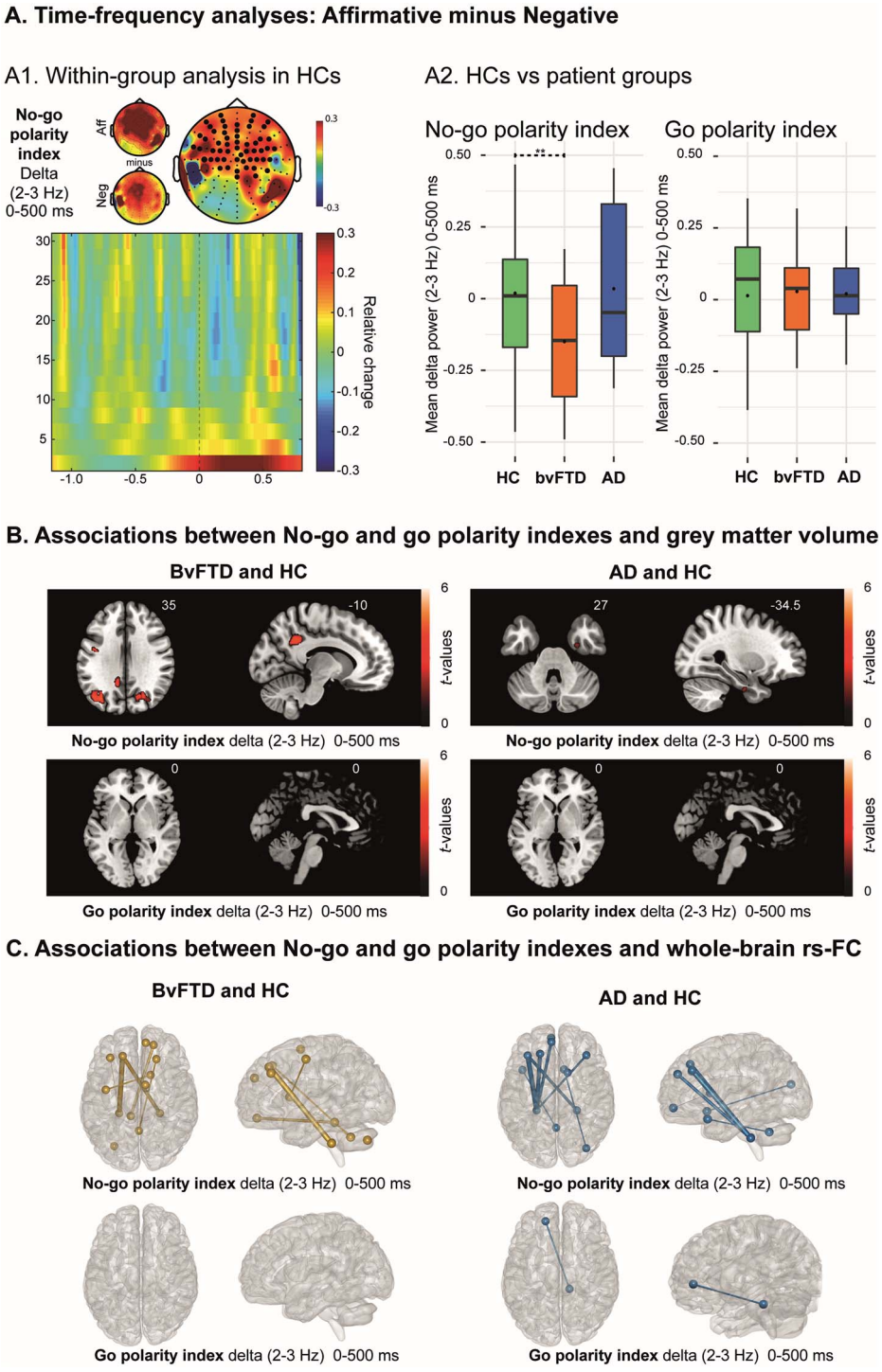

Fig. 2. (A) Time–frequency analyses for polarity (affirmative vs negative trials). (A1). Significant spatiotemporal cluster from the comparison between affirmative and negative No-go trials (No-go polarity index) for the delta band (2–3 Hz) in HCs. (A2) Between groups comparisons for the mean No-go polarity and the Go polarity indexes, respectively. The dashed line represents the significant difference between HCs and the bvFTD group ($P < 0.01$). (B) Associations between No-go and Go polarity indexes and gray matter volume. For the bvFTD and HC tandem, the No-go polarity index was positively associated with gray matter volume of the left medial–posterior cingulum, precentral gyrus, and angular gyrus, as well as the left midinferior and right superior occipital cortices (top left inset); instead, the Go polarity index presented no significant associations (bottom left inset). For the AD and HC tandem, the No-go polarity index was significantly associated with the volume of the right fusiform gyrus (top right inset); instead, the Go polarity index presented no significant associations (bottom right inset). (C) Associations between No-go and Go polarity indexes and rs-FC. For the bvFTD and the HC tandem, the No-go polarity index was associated with connectivity between frontocerebellar regions (top left inset); instead, the Go polarity index presented no significant associations (bottom left inset). For the AD and HC tandem, the No-go polarity index was associated with connectivity of frontocerebellar regions as well as occipital and temporal areas (top right inset); contrariwise, the Go-polarity index also correlated with connectivity between frontocerebellar regions (bottom right inset). Results were obtained from whole-brain analyses over 90 regions of interest, considering an uncorrected $P < 0.001$. Link thickness indicates connectivity strength.

group. First, in the bvFTD-HC tandem, the No-go polarity index was positively associated with gray matter volume of the left medial–posterior cingulum, precentral gyrus, and angular gyrus, as well as the left midinferior and right superior occipital cortices (Fig. 2B, top left inset). No significant associations were found between the Go polarity index and gray matter volume (Fig. 2B, bottom left inset). Second, in the AD-HC index, the No-go polarity index was significantly associated with the volume of the right fusiform gyrus (Fig. 2B, top right inset). No association was found between the Go polarity index and the volume of any brain area (Fig. 2B, bottom right, inset). For details, see Supplementary Material 7, Table S7.

Associations between oscillatory indices and fMRI resting-state connectivity

Each patient group showed different associations between oscillatory indices and fMRI connectivity patterns. First, in the bvFTD-HC tandem, the No-go polarity index was associated with connectivity between (i) the bilateral superior frontal gyrus and bilateral cerebellar regions, (ii) frontal/prefrontal (midfrontal and superior orbital) regions and the left cerebellum, (iii) the superior motor area and the left cerebellum, (iv) the right precentral gyrus and the caudate nucleus, and (v) the supplementary motor area and cerebellum (Fig. 2C, top left inset). In contrast, the Go polarity index was not significantly associated with any connectivity pattern (Fig. 2C, bottom left inset). Second, in the AD-HC tandem, the No-go polarity index was associated with connectivity between (i) the left superior frontal gyrus and the left cerebellum, (ii) the midsuperior frontal cortex and the left cerebellum, (iii) the bilateral medial frontal cortex and the bilateral cerebellum, (iv) the midorbital frontal cortex and the right caudate nucleus, (v) the right olfactory area and the right medial occipital cortex, and (vi) the left superior temporal cortex and the vermis (Fig. 2C, top right inset). Also, the Go polarity index was associated with connectivity between the left superior orbital cortex and the right cerebellum, suggesting nonspecific relations with inhibitory processes (Fig. 2C, bottom right inset). Briefly, the bvFTD group showed frontocerebellar associations restricted to the No-go polarity index only. On the other hand, AD presented widespread anteroposterior associations with the No-go polarity index, comprising frontocerebellar, occipital, and temporal areas; moreover, it presented frontocerebellar associations with the Go polarity index. For details, see Supplementary Material 8.

Discussion

This multilevel study examined the interplay of negation and inhibition in strategic neurodegenerative models. In HCs, negation distinctly suppressed frontocentral delta power, a canonical inhibitory marker. This modulation, along with canonical oscillatory signatures of motor inhibition, was abolished in bvFTD but not in AD patients. Moreover, disruptions of the No-go polarity index over the delta band in bvFTD correlated with anatomofunctional patterns mainly implicating inhibitory regions (precentral gyrus and frontocerebellar networks). Though preliminary due to the study's sample size, our results suggest that multidimensional inhibitory mechanisms are involved in negation processing and point to potential disease-differential markers of bvFTD.

The No-go polarity index showed greater delta power for affirmative than negative sentences, indicating delta suppression for the latter. No such effect was observed in other bands or in the Go polarity index. This supports the involvement of inhibitory mechanisms during negation processing. In fact, delta activity is a canonical signature of inhibitory processing, being typically reduced during response suppression (Harmony 2013; Huster et al. 2013) and significantly modulated during cognitive (Cooper et al. 2016) and affective (Benvenuti et al. 2017) inhibition. Intriguingly, prior studies with the same task in healthy participants found similar effects only in the theta and beta bands (de Vega et al. 2016; Beltrán et al. 2019). However, these studies focused on young populations, while the present work targeted elderly subjects. As argued below, this might reflect differences in the sensitivity of theta and delta modulations during inhibition across the lifespan (Kolev et al. 2009; Schmiedt-Fehr and Basar-Eroglu 2011). Compatibly, our study suggests that this inhibitory marker may be a crucial correlate of negation processing in late adulthood.

Such specific delta marker was altered only in bvFTD. As confirmed by motor inhibition EEG results, this disease presents early inhibitory disruptions (Rascovsky et al. 2011) affecting not only bodily action (Hughes et al. 2015) but also cognitive (Hornberger et al. 2008) and socioemotional (Ibáñez 2018; Godefroy et al. 2021) domains. To our knowledge, delta oscillations have not been previously studied during inhibition in bvFTD. However, their sensitivity to inhibitory disruptions has been validated in other populations exhibiting high impulsivity and socially inadequate behavior, including bipolar (Atagün et al. 2014) and schizophrenic (Ergen et al. 2008; Ford et al. 2008) patients, and alcoholic individuals with suspected frontal damage (Kamarajan et al. 2004; Pandey et al. 2016). Similar disinhibited behavior has been reported in bvFTD (Young et al. 2010; Rascovsky et al. 2011; Baez et al. 2014). Thus, the No-go polarity index in bvFTD patients suggests that their abnormal negation reflects disrupted inhibitory mechanisms. In this sense, the multidomain behavior-suppression disruptions characterizing bvFTD seem to affect linguistic processes, potentially revealing new forms of altered cognitive inhibition.

Compatibly, in the bvFTD-HC tandem, this No-go polarity index was associated with the volume of the precentral and angular gyri, alongside the medial posterior cingulum and the middle occipital cortex, linked to motor (Chambers et al. 2009; Huster et al. 2013), cognitive (Langenecker et al. 2004;

Bernal and Altman 2009), and socioemotional (Hung et al. 2018; Ibáñez 2018) inhibition, as well as negation processing (Tettamanti et al. 2008; Christensen 2009; Bahlmann et al. 2011). Congruently, the No-go polarity index correlated with rs-FC between key areas implicated in inhibition, such as superior and prefrontal regions (Karch et al. 2008; Beltrán et al. 2018), the caudate nucleus (Chambers et al. 2009), and the cerebellum (Zheng et al. 2008; Mannarelli et al. 2020). Importantly, some such structures are also implicated in negation—e.g. midsuperior motor and left precentral areas (Tettamanti et al. 2008; Christensen 2009; Tomasino et al. 2010; Bahlmann et al. 2011). These patterns were absent in the Go polarity index, which might suggest that multilevel alterations of negation processing emerged only when response suppression mechanisms were engaged. Briefly, the integration of both domains seems to be distinctly and cross-dimensionally disrupted in patients with primary inhibitory deficits.

Indeed, selective oscillatory disruptions were absent in AD patients, who also exhibited preserved EEG signatures during motor inhibition. While AD often involves disinhibitory manifestations, these are neither systematic nor diagnostic (Kramer et al. 2003; Stopford et al. 2012), which might account for such partly preserved marker. Indeed, in this group, the No-go polarity index correlated with the volume of the right fusiform gyrus, a region typically implicated in lexicosemantic deficits across AD cohorts (Kuperberg et al. 2000; Forseth et al. 2018). The potential role of such domain in the disruptions of AD patients is reinforced by the magnitude of their deficits in the Hayling test (Table 1), which hinges heavily on lexicosemantic systems (Belleville et al. 2006) that are commonly impaired in this population (Bondi et al. 2002; Nestor et al. 2006). Moreover, the No-go polarity index in AD patients was mainly associated with frontocerebellar networks as well as temporal and occipital hubs. Given that the No-go polarity index was preserved, such associations might be driven by overall cognitive demands, which, in AD, involve reduced delta activity (Yener et al. 2008; Başar and Güntekin 2013) and modulations along frontocerebellar regions (Zheng et al. 2017; Jacobs et al. 2018). In fact, frontocerebellar networks in AD also correlated with the Go polarity index, highlighting the lack of distinct associations with inhibition. Briefly, the neural integration of negation and inhibition might be differentially disrupted in persons typified by primary inhibitory deficits (namely, bvFTD patients).

From a theoretical stance, this study supports the "reuse of inhibition for negation" framework (Beltrán et al. 2021), but its results might enable alternative interpretations. Indeed, delta and/or theta suppression has also been related to attentional (Harmony 2013) and working memory (Polich 2007; Harper et al. 2014) functions, both of which may be more markedly taxed during No-go than during Go trials (O'Connell et al. 2009; Redick et al. 2011; Chen and Cave 2016; Harper et al. 2016). Moreover, these domains have been linked to some of the brain regions and networks captured in our correlations results (Criaud and Boulinguez 2013; Yaple et al. 2019). Accordingly, the inhibitory mechanisms we postulate may be accompanied by other associated effects. That being said, the study's design and multidimensional results strongly converge to support the proposed interpretation. Indeed, our main findings (i) pertain to the No-go polarity (as opposed to the Go polarity) condition; (ii) replicate previous EEG findings motivating our hypotheses (de Vega et al. 2016; Beltrán et al. 2019); (iii) reveal selective alterations in that condition only for patients with primary inhibitory disorders (bvFTD), as opposed to those with nondiagnostic inhibitory difficulties (AD); and (iv) correlate with regions and networks that are systematically linked to inhibition in the literature. Notwithstanding, future research could incorporate specific manipulations to ascertain the role of other functions that might mediate the observed results, disentangling possible competing explanations.

At the same time, this study challenges recent localizationist views linking negation to a single putative area (in the anterior insula) specialized for nonverbal logical processes (Grodzinsky et al. 2020). In particular, Grodzinsky et al. (2020, 29) interpret their findings on negation as evidence "that the border between the insula and Broca's region is where language stops and logic begins." Conversely, we found that key negation markers are associated with fronto-striato-cerebellar circuits, supporting network-based accounts of neurocognition (Mišić and Sporns 2016). Moreover, by demonstrating that core mechanisms subserving (nonverbal) inhibition are involved in processing (verbal) negation, our findings suggest that the latter function operates *at the crossing* of linguistic and nonlinguistic systems, further clashing against modularist accounts.

Moreover, while previous EEG reports linking negation with inhibition observed theta-band modulations in adults (de Vega et al. 2016; Beltrán et al. 2019), our work revealed oscillatory correlates of negation in the delta band for elderly participants. However, theta band activity was, indeed, associated with *motor* inhibition, replicating previous works (Nigbur et al. 2011; Huster et al. 2013). This indicates that, at least in elderly persons, the inhibitory mechanisms mediating physical action suppression may not be identical to those subserving sentential negation. Thus, as suggested elsewhere (Kolev et al. 2009; Schmiedt-Fehr and Basar-Eroglu 2011), theta and delta oscillations may become differentially (in)sensitive to relevant processes throughout aging. This finding motivates a new ontogenetic hypothesis, suggesting that critical signatures of negation may adapt to age-related neural profiles, as observed for lexeme retrieval (den Hollander et al. 2019), word anticipation (Wlotko et al. 2012; Broderick et al. 2021), and sentence comprehension (Wingfield and Grossman 2006).

Interestingly, neurophysiological disruptions of the No-go polarity index were not mirrored by behavioral results, as in previous reports of the same task

(de Vega et al. 2016; Beltrán et al. 2019). The same was true for the motor inhibition index, replicating the absence of behavioral deficits in Go/No-go tasks and other motor inhibition paradigms for both bvFTD (Dimitrov et al. 2003; Collette et al. 2007; Hughes et al. 2018) and AD (Collette et al. 2007). These patterns align with language grounding research capturing neural effects alongside null behavioral signatures (e.g. Kiefer et al. 2008; Willems et al. 2010; Hauk and Tschentscher 2013; Dalla Volta et al. 2018; García et al. 2019). Similarly, our task seems sensitive to fine-grained neural effects, which may not be mirrored behaviorally, inviting further research with alternative paradigms.

Finally, from a clinical perspective, negation tasks could reveal differential markers across neurodegenerative disorders. Previous works have leveraged other linguistic materials, such as emotion-laden sentences (Santamaría-García et al. 2017) or action-laden texts (Moguilner et al. 2021), to capture discriminatory neural markers of diseases presenting different brain disturbances. Tentatively, our results point to negation as a promising target for bvFTD, reinforcing the value of linguistic assessments for differential characterizations of the disease (Hardy et al. 2016; Geraudie, Díaz Rivera, et al. 2021b). More generally, while previous clinical research on inhibition has focused on motoric (Collette et al. 2007), cognitive (Hornberger et al. 2008), and affective (Godefroy et al. 2021) dimensions, these findings open a new avenue to capture (dis)inhibitory dynamics elicited by negation. As seen in other studies on bvFTD (Santamaría-García et al. 2017; Legaz et al. 2021), broadening the canonical dimensions of a critical domain can reveal nosological distinctions and favor more fine-grained phenotyping.

Limitations and avenues for further research

Our study presents some limitations. First, the sample sizes are modest. Although these *N*s match those of previous reports yielding replicable findings (Hughes et al. 2011; Premi et al. 2014) and mirror the size of multiple bvFTD reports assessing language (Geraudie, Battista, et al. 2021a), inhibition (Dimitrov et al. 2003; Hornberger et al. 2010; Hornberger et al. 2011; O'Callaghan et al. 2013; Santillo et al. 2016), and other domains (Farag et al. 2010; Mendez and Shapira 2011; Agosta et al. 2012; Couto et al. 2013; Filippi et al. 2013; Henry et al. 2014; Nasseroleslami et al. 2019; Pasquini et al. 2020), further studies should test our approach with more participants to ensure better statistical power and more robust effects. Second, since our task did not require fast-paced key presses, the need to suppress prepotent responses on No-go trials was not at its highest. While this promoted task feasibility for patients, further works should employ alternative tasks with more stringent action-suppression demands. Third, the No-go polarity index may be partly influenced by other mechanisms related to response inhibition, such as conflict monitoring or error detection (Harper et al. 2016). Future studies should develop new paradigms to disentangle inhibition- and control-related processes underlying negation comprehension.

Also, our work leads to novel research questions. We have surmised that delta and theta modulations might be differentially sensitive to inhibitory dynamics in younger and elderly populations. Direct testing of this hypothesis, via comparisons between participants from different age groups, could open a lifespan perspective on the neural mechanisms underpinning negation processing. Additionally, while we focused on negated action verbs, future studies should examine whether bvFTD patients present similar disruptions during negation of abstract verbs (Beltrán et al. 2019). Also, the atrophy pattern of the bvFTD sample corresponded to a temporal subtype. Although inhibitory alterations are prominent in this presentation (Whitwell et al. 2009; Ranasinghe et al. 2016) and are often associated to temporal atrophy (Liu et al. 2004; Zamboni et al. 2008; Chan et al. 2009; Whitwell et al. 2009; Ranasinghe et al. 2016) and hypoperfusion (Ber et al. 2006; McMurtray et al. 2006) across bvFTD cohorts, it would be vital to replicate our work on bvFTD patients typified by more canonical frontal disruptions. Finally, since our imaging protocol did not include active paradigms, task-related EEG modulations could only be correlated with offline MRI/fMRI measures. Future studies could replicate our work with online imaging recordings.

Conclusion

In conclusion, this is the first study examining multidimensional neurocognitive links between negation and inhibition across neurodegenerative diseases. Canonical oscillatory signatures of inhibition during negation processing were selectively disrupted in bvFTD (but not AD) patients and related to anatomofunctional properties of inhibitory regions. Our results indicate that negation hinges on the *integrity and interaction* of spatiotemporal inhibitory mechanisms while potentially revealing differential markers of neurodegenerative dementias. Further research along these lines may inspire basic and translational breakthroughs across neuroscientific and clinical fields.

Author contributions

Mariano N. Díaz-Rivera: Methodology, Investigation, Data Curation, Formal Analysis, Writing—original draft preparation, Visualization. Agustina Birba: Methodology, Investigation, Formal Analysis, Writing—original draft preparation, Visualization. Sol Fittipaldi: Software, Data Curation, Formal analysis, Visualization. Débora Mola: Data Curation. Yurena Morera: Software, Data Curation. Manuel de Vega: Conceptualization, Software, Investigation. Sebastian Moguilner: Formal analysis. Patricia Lillo: Resources, Data Curation. Andrea Slachevsky: Resources, Data curation. Cecilia González Campo: Software, Data Curation, Formal analysis, Visualization. Agustín Ibáñez:

Conceptualization, Methodology, Resources, Writing—review & editing, Project administration, Funding acquisition. Adolfo M. García Conceptualization, Methodology, Resources, Writing—original draft preparation, Writing—review & editing, Visualization, Supervision, Project administration, Funding acquisition.

Acknowledgments

We extend our deepest gratitude to all patients and their families, who disinterestedly offered their valuable time to the study. We thankfully acknowledge the collaboration of Instituto Conci Carpinella (Córdoba, Argentina), Hospital Nacional de Clínicas (Facultad de Ciencias Médicas, Universidad Nacional de Córdoba, Córdoba, Argentina), the Memory and Neuropsychiatric Clinic (CMYN) (Neurology Department, Hospital del Salvador and Facultad de Medicina, University of Chile, Santiago, Chile), and the Neuroradiologic Department (Instituto de Neurocirugía Asenjo, Santiago, Chile). Corresponding author address: Adolfo M. García, PhD, Universidad de San Andrés & CONICET; Vito Dumas 284, B1644BID Victoria, Buenos Aires, Argentina.

Supplementary material

Supplementary material is available at *Cerebral Cortex Journal* online.

Funding

This work was supported by CONICET and FONCYT-PICT [grant numbers 2017-1818, 2017-1820]. Manuel de Vega and Yurena Morera are funded by the Spanish Ministerio de Ciencia, Innovación y Universidades, and by the European Regional Development Funds (Grant RTI2018-098730-B-I00). Patricia Lillo is supported by grants for ANID, FONDAP [15150012] and ANID, FONDECYT regular [1160940]. Andrea Slachevsky is supported by grants from ANID/FONDAP/15150012; ANID, FONDEF [18I10113]; and ANID, FONDECYT [1191726]. Agustín Ibáñez is supported by grants of Alzheimer's Association GBHI ALZ UK-20-639295; Takeda CW2680521; ANIDANID/FONDECYT Regular (1210195); ANID/FONDAP 15150012, Sistema General de Regalías [BPIN2018000100059], Universidad del Valle [CI 5316], and the Multi-Partner Consortium to Expand Dementia Research in Latin America (ReDLat), funded by the National Institutes of Aging (NIA) of the National Institutes of Health (NIH) under award number R01AG057234, an Alzheimer's Association grant (SG-20-725707-ReDLat), the Rainwater Foundation, and the Global Brain Health Institute. Adolfo García is an Atlantic Fellow at the Global Brain Health Institute (GBHI) and is supported with funding from GBHI, Alzheimer's Association, and Alzheimer's Society (Alzheimer's Association GBHI ALZ UK-22-865742); ANID, FONDECYT Regular [1210176]; and Programa Interdisciplinario de Investigación Experimental en Comunicación y Cognición (PIIECC), Facultad de Humanidades, USACH. The content is solely the responsibility of the authors and does not represent the official views of the National Institutes of Health, Alzheimer's Association, Rainwater Charitable Foundation, or Global Brain Health Institute.

Conflict of interest statement. No author has any conflict of interest to report.

Competing interests

Mariano N. Díaz-Rivera: The author declares no competing financial interests. Agustina Birba: The author declares no competing financial interests. Sol Fittipaldi: The author declares no competing financial interests. Débora Mola: The author declares no competing financial interests. Yurena Morera: The author declares no competing financial interests. Manuel de Vega: The author declares no competing financial interests. Sebastian Moguilner: The author declares no competing financial interests. Patricia Lillo: The author declares no competing financial interests. Andrea Slachevsky: The author declares no competing financial interests. Cecilia González Campo: The author declares no competing financial interests. Agustín Ibáñez: The author declares no competing financial interests. Adolfo M. García: The author declares no competing financial interests.

Data availability

All experimental data and the scripts used are fully available online via the Open Science Framework at https://osf.io/n2abf/?view_only=3a56a65940db440f9c5af4ce88fb93f2 (data from "Multidimensional inhibitory signatures of sentential negation in neurodegenerative disorders").

References

Agosta F, Scola E, Canu E, Marcone A, Magnani G, Sarro L, Copetti M, Caso F, Cerami C, Comi G, et al. White matter damage in frontotemporal lobar degeneration spectrum. *Cereb Cortex*. 2012:22:2705–2714.

Aravena P, Delevoye-Turrell Y, Deprez V, Cheylus A, Paulignan Y, Frak V, Nazir T. Grip force reveals the context sensitivity of language-induced motor activity during "action words" processing: evidence from sentential negation. *PLoS One*. 2012:7:e50287.

Aron AR, Poldrack RA. Cortical and subcortical contributions to stop signal response inhibition: role of the subthalamic nucleus. *J Neurosci*. 2006:26:2424–2433.

Ashburner J, Friston KJ. Nonlinear spatial normalization using basis functions. *Hum Brain Mapp*. 1999:7:254–266.

Ashburner J, Friston KJ. Voxel-based morphometry—the methods. *NeuroImage*. 2000:11:805–821.

Atagün Mİ, Güntekin B, Maşalı B, Tülay E, Başar E. Decrease of event-related delta oscillations in euthymic patients with bipolar disorder. *Psychiatry Res Neuroimaging*. 2014:223:43–48.

Bachli MB, Sedeño L, Ochab JK, Piguet O, Kumfor F, Reyes P, Torralva T, Roca M, Cardona JF, Campo CG, et al. Evaluating the reliability of neurocognitive biomarkers of neurodegenerative diseases across countries: a machine learning approach. *NeuroImage*. 2020:208:116456.

Baez S, Couto B, Torralva T, Sposato LA, Huepe D, Montañes P, Reyes P, Matallana D, Vigliecca NS, Slachevsky A, et al. Comparing moral judgments of patients with frontotemporal dementia and frontal stroke. *JAMA Neurol*. 2014:71:1172–1176.

Bahlmann J, Mueller JL, Makuuchi M, Friederici AD. Perisylvian functional connectivity during processing of sentential negation. *Front Psychol*. 2011:2:104.

Başar E, Güntekin B. Review of delta, theta, alpha, beta, and gamma response oscillations in neuropsychiatric disorders. *Suppl Clin Neurophysiol*. 2013:62:303–341.

Belleville S, Rouleau N, Van der Linden M. Use of the Hayling task to measure inhibition of prepotent responses in normal aging and Alzheimer's disease. *Brain Cogn*. 2006:62:113–119.

Beltrán D, Liu B, de Vega M. Inhibitory mechanisms in the processing of negations: a neural reuse hypothesis. *J Psycholinguist Res*. 2021:50:1243–1260.

Beltrán D, Muneton-Ayala M, de Vega M. Sentential negation modulates inhibition in a stop-signal task. Evidence from behavioral and ERP data. *Neuropsychologia*. 2018:112:10–18.

Beltrán D, Morera Y, García-Marco E, Vega MD. Brain inhibitory mechanisms are involved in the processing of sentential negation, regardless of its content. Evidence from EEG theta and beta rhythms. *Front Psychol*. 2019:10:1782.

Benvenuti SM, Buodo G, Palomba D. Appetitive and aversive motivation in dysphoria: a time-domain and time-frequency study of response inhibition. *Biol Psychol*. 2017:125:12–27.

Ber IL, Guedj E, Gabelle A, Verpillat P, Volteau M, Thomas-Anterion C, Decousus M, Hannequin D, Vera P, Lacomblez L. Demographic, neurological and behavioural characteristics and brain perfusion SPECT in frontal variant of frontotemporal dementia. *Brain*. 2006:129:3051–3065.

Bernal B, Altman N. Neural networks of motor and cognitive inhibition are dissociated between brain hemispheres: an fMRI study. *Int J Neurosci*. 2009:119:1848–1880.

Birba A, García-Cordero I, Kozono G, Legaz A, Ibanez A, Sedeno L, García AM. Losing ground: frontostriatal atrophy disrupts language embodiment in Parkinson's and Huntington's disease. *Neurosci Biobehav Rev*. 2017:80:673–687.

Birba A, Beltrán D, Martorell Caro M, Trevisan P, Kogan B, Sedeño L, Ibáñez A, García AM. Motor-system dynamics during naturalistic reading of action narratives in first and second language. *NeuroImage*. 2020:216:116820.

Birba A, Fittipaldi S, Cediel Escobar J, Gonzalez Campo C, Legaz A, Galiani A, Díaz Rivera M, Martorell Caro M, Alifano F, Piña-Escudero S, et al. Multimodal neurocognitive markers of naturalistic discourse typify diverse neurodegenerative diseases. *Cereb Cortex*. 2021:bhab421. https://doi.org/10.1093/cercor/bhab421.

Bondi MW, Serody AB, Chan AS, Eberson-Shumate SC, Delis DC, Hansen LA, Salmon DP. Cognitive and neuropathologic correlates of Stroop color-word test performance in Alzheimer's disease. *Neuropsychology*. 2002:16:335.

Broderick MP, Di Liberto GM, Anderson AJ, Rofes A, Lalor EC. Dissociable electrophysiological measures of natural language processing reveal differences in speech comprehension strategy in healthy ageing. *Sci Rep*. 2021:11:4963.

Burgess PW, Shallice T. *The hayling and brixton tests*. Bury St Edmunds: Thames Valley Test Company. 1997.

Burton EJ, McKeith IG, Burn DJ, Williams ED, O'Brien JT. Cerebral atrophy in Parkinson's disease with and without dementia: a comparison with Alzheimer's disease, dementia with Lewy bodies and controls. *Brain*. 2004:127:791–800.

Cervetto S, Díaz-Rivera M, Petroni A, Birba A, Caro MM, Sedeño L, Ibáñez A, García AM. The neural blending of words and movement: event-related potential signatures of semantic and action processes during motor–language coupling. *J Cogn Neurosci*. 2021:33:1–15.

Chambers CD, Garavan H, Bellgrove MA. Insights into the neural basis of response inhibition from cognitive and clinical neuroscience. *Neurosci Biobehav Rev*. 2009:33:631–646.

Chan D, Anderson V, Pijnenburg Y, Whitwell J, Barnes J, Scahill R, Stevens JM, Barkhof F, Scheltens P, Rossor MN. The clinical profile of right temporal lobe atrophy. *Brain*. 2009:132:1287–1298.

Chan D, Walters R, Sampson E, Schott J, Smith S, Rossor M. EEG abnormalities in frontotemporal lobar degeneration. *Neurology*. 2004:62:1628–1630.

Chao-Gan Y, Yu-Feng Z. DPARSF: a MATLAB toolbox for "pipeline" data analysis of resting-state fMRI. *Front Syst Neurosci*. 2010:4:13.

Chen Z, Cave KR. Zooming in on the cause of the perceptual load effect in the go/no-go paradigm. *J Exp Psychol Hum Percept Perform*. 2016:42:1072.

Christensen KR. Negative and affirmative sentences increase activation in different areas in the brain. *J Neurolinguistics*. 2009:22:1–17.

Collette F, Van der Linden M, Delrue G, Salmon E. Frontal hypometabolism does not explain inhibitory dysfunction in Alzheimer disease. *Alzheimer Dis Assoc Disord*. 2002:16:228–238.

Collette F, Amieva H, Adam S, Hogge M, Van der Linden M, Fabrigoule C, Salmon E. Comparison of inhibitory functioning in mild Alzheimer's disease and frontotemporal dementia. *Cortex*. 2007:43:866–874.

Cooper PS, Darriba Á, Karayanidis F, Barceló F. Contextually sensitive power changes across multiple frequency bands underpin cognitive control. *NeuroImage*. 2016:132:499–511.

Courellis HS, Iversen JR, Poizner H, Cauwenberghs G. EEG channel interpolation using ellipsoid geodesic length. In: *2016 IEEE biomedical circuits and systems conference (BioCAS)*. IEEE; 2016. pp. 540–543 https://ieeexplore.ieee.org/document/7833851.

Couto B, Manes F, Montanes P, Matallana D, Reyes P, Velasquez M, Yoris A, Baez S, Ibanez A. Structural neuroimaging of social cognition in progressive non-fluent aphasia and behavioral variant of frontotemporal dementia. *Front Hum Neurosci*. 2013:7:467.

Criaud M, Boulinguez P. Have we been asking the right questions when assessing response inhibition in go/no-go tasks with fMRI? A meta-analysis and critical review. *Neurosci Biobehav Rev*. 2013:37:11–23.

Dalla Volta R, Avanzini P, De Marco D, Gentilucci M, Fabbri-Destro M. From meaning to categorization: the hierarchical recruitment of brain circuits selective for action verbs. *Cortex*. 2018:100:95–110.

Dehaene S, Cohen L. Cultural recycling of cortical maps. *Neuron*. 2007:56:384–398.

de la Fuente A, Sedeño L, Vignaga SS, Ellmann C, Sonzogni S, Belluscio L, García-Cordero I, Castagnaro E, Boano M, Cetkovich M. Multimodal neurocognitive markers of interoceptive tuning in smoked cocaine. *Neuropsychopharmacology*. 2019:44:1425–1434.

de Vega M, Morera Y, Leon I, Beltrán D, Casado P, Martin-Loeches M. Sentential negation might share neurophysiological mechanisms with action inhibition. Evidence from frontal theta rhythm. *J Neurosci*. 2016:36:6002–6010.

den Hollander J, Jonkers R, Mariën P, Bastiaanse R. Identifying the speech production stages in early and late adulthood by using electroencephalography. *Front Hum Neurosci*. 2019:13:298. https://doi.org/10.3389/fnhum.2019.00298.

Dimitrov M, Nakic M, Elpern-Waxman J, Granetz J, O'Grady J, Phipps M, Milne E, Logan GD, Hasher L, Grafman J. Inhibitory attentional control in patients with frontal lobe damage. *Brain Cogn*. 2003:52: 258–270.

Donix M, Jurjanz L, Meyer S, Amanatidis EC, Baeumler D, Huebner T, Poettrich K, Smolka MN, Holthoff VA. Functional imaging during recognition of personally familiar faces and places in Alzheimer's disease. *Arch Clin Neuropsychol*. 2013:28:72–80.

Donnelly-Kehoe PA, Pascariello GO, García AM, Hodges JR, Miller B, Rosen H, Manes F, Landin-Romero R, Matallana D, Serrano C, et al. Robust automated computational approach for classifying frontotemporal neurodegeneration: multimodal/-multicenter neuroimaging. *Alzheimers Dement (Amst)*. 2019:11: 588–598.

Dottori M, Hesse E, Santilli M, Vilas MG, Caro MM, Fraiman D, Sedeño L, Ibáñez A, García AM. Task-specific signatures in the expert brain: differential correlates of translation and reading in professional interpreters. *NeuroImage*. 2020:209:116519.

Ergen M, Marbach S, Brand A, Başar-Eroğlu C, Demiralp T. P3 and delta band responses in visual oddball paradigm in schizophrenia. *Neurosci Lett*. 2008:440:304–308.

Farag C, Troiani V, Bonner M, Powers C, Avants B, Gee J, Grossman M. Hierarchical organization of scripts: converging evidence from FMRI and frontotemporal degeneration. *Cereb Cortex*. 2010:20: 2453–2463.

Filippi M, Agosta F, Scola E, Canu E, Magnani G, Marcone A, Valsasina P, Caso F, Copetti M, Comi G. Functional network connectivity in the behavioral variant of frontotemporal dementia. *Cortex*. 2013:49:2389–2401.

Fittipaldi S, Abrevaya S, de la Fuente A, Pascariello GO, Hesse E, Birba A, Salamone P, Hildebrandt M, Martí SA, Pautassi R, et al. A multidimensional and multi-feature framework for cardiac interoception. *NeuroImage*. 2020:212:116677.

Ford JM, Roach BJ, Hoffman RS, Mathalon DH. The dependence of P300 amplitude on gamma synchrony breaks down in schizophrenia. *Brain Res*. 2008:1235:133–142.

Foroni F, Semin GR. Comprehension of action negation involves inhibitory simulation. *Front Hum Neurosci*. 2013:7:209.

Forseth KJ, Kadipasaoglu CM, Conner CR, Hickok G, Knight RT, Tandon N. A lexical semantic hub for heteromodal naming in middle fusiform gyrus. *Brain*. 2018:141:2112–2126.

Frossard & Renaud. Permutation Tests for Regression, ANOVA, and Comparison of Signals: The permuco Package. *Journal of Statistical Software*. 2021:99(15):1–32. https://doi.org/10.18637/jss.v099.i15.

García AM, Moguilner S, Torquati K, García-Marco E, Herrera E, Muñoz E, Castillo EM, Kleineschay T, Sedeño L, Ibáñez A. How meaning unfolds in neural time: embodied reactivations can precede multimodal semantic effects during language processing. *NeuroImage*. 2019:197:439–449.

García AM, Hesse E, Birba A, Adolfi F, Mikulan E, Caro MM, Petroni A, Bekinschtein TA, del Carmen García M, Silva W, et al. Time to face language: embodied mechanisms underpin the inception of face-related meanings in the human brain. *Cereb Cortex*. 2020:30: 6051–6068.

García-Cordero I, Sedeño L, de la Fuente L, Slachevsky A, Forno G, Klein F, Lillo P, Ferrari J, Rodriguez C, Bustin J, et al. Feeling, learning from and being aware of inner states: interoceptive dimensions in neurodegeneration and stroke. *Phil Trans R Soc B Biol Sci*. 2016:371:20160006.

García-Cordero I, Esteves S, Mikulan EP, Hesse E, Baglivo FH, Silva W, García MC, Vaucheret E, Ciraolo C, García HS, et al. Attention, in and out: scalp-level and intracranial EEG correlates of interoception and exteroception. *Front Neurosci*. 2017:11:411.

García-Cordero I, Sedeño L, Babino A, Dottori M, Melloni M, Martorell Caro M, Sigman M, Herrera E, Manes F, García AM, et al. Explicit and implicit monitoring in neurodegeneration and stroke. *Sci Rep*. 2019:9:14032.

García-Cordero I, Migeot J, Fittipaldi S, Aquino A, Campo CG, García A, Ibáñez A. Metacognition of emotion recognition across neurodegenerative diseases. *Cortex*. 2021:137:93–107.

García-Marco E, Morera Y, Beltrán D, de Vega M, Herrera E, Sedeño L, Ibáñez A, García AM. Negation markers inhibit motor routines during typing of manual action verbs. *Cognition*. 2019:182: 286–293.

Geraudie A, Battista P, García AM, Allen IE, Miller ZA, Gorno-Tempini ML, Montembeault M. Speech and language impairments in behavioral variant frontotemporal dementia: a systematic review. *Neurosci Biobehav Rev*. 2021a:131:1076–1095.

Geraudie A, Díaz Rivera M, Montembeault M, García AM. Language in Behavioral variant frontotemporal dementia: another stone to be turned in Latin America. *Front Neurol*. 2021b:12: 702770.

Godefroy V, Tanguy D, Bouzigues A, Sezer I, Ferrand-Verdejo J, Azuar C, Bendetowicz D, Carle G, Rametti-Lacroux A, Bombois S. Frontotemporal dementia subtypes based on behavioral inhibition deficits. *Alzheimers Dement*. 2021:13:e12178.

Good CD, Johnsrude IS, Ashburner J, Henson RN, Friston KJ, Frackowiak RS. A voxel-based morphometric study of ageing in 465 normal adult human brains. *NeuroImage*. 2001:14:21–36.

Grodzinsky Y, Deschamps I, Pieperhoff P, Iannilli F, Agmon G, Loewenstein Y, Amunts K. Logical negation mapped onto the brain. *Brain Struct Funct*. 2020:225:19–31.

Hardy CJ, Buckley AH, Downey LE, Lehmann M, Zimmerer VC, Varley RA, Crutch SJ, Rohrer JD, Warrington EK, Warren JD. The language profile of behavioral variant frontotemporal dementia. *J Alzheimers Dis*. 2016:50:359–371.

Harmony T. The functional significance of delta oscillations in cognitive processing. *Front Integr Neurosci*. 2013:7:83.

Harper J, Malone SM, Bernat EM. Theta and delta band activity explain N2 and P3 ERP component activity in a go/no-go task. *Clin Neurophysiol*. 2014:125:124–132.

Harper J, Malone SM, Bachman MD, Bernat EM. Stimulus sequence context differentially modulates inhibition-related theta and delta band activity in a go/no-go task. *Psychophysiology*. 2016:53: 712–722.

Hauk O, Tschentscher N. The body of evidence: what can neuroscience tell us about embodied semantics? *Front Psychol*. 2013:4:50.

Hayes AF. Permutation test is not distribution-free: testing H_o: $\rho = 0$. *Psychol Methods*. 1996:1:184–198.

Henry JD, Phillips LH, Von Hippel C. A meta-analytic review of theory of mind difficulties in behavioural-variant frontotemporal dementia. *Neuropsychologia*. 2014:56:53–62.

Horn L. *A natural history of negation* Chicago: The University of Chicago Press, 1989.

Hornberger M, Piguet O, Kipps C, Hodges JR. Executive function in progressive and nonprogressive behavioral variant frontotemporal dementia. *Neurology*. 2008:71:1481–1488.

Hornberger M, Savage S, Hsieh S, Mioshi E, Piguet O, Hodges J. Orbitofrontal dysfunction discriminates behavioral variant frontotemporal dementia from Alzheimer's disease. *Dement Geriatr Cogn Disord*. 2010:30:547–552.

Hornberger M, Geng J, Hodges JR. Convergent grey and white matter evidence of orbitofrontal cortex changes related to disinhibition in behavioural variant frontotemporal dementia. *Brain*. 2011:134: 2502–2512.

Hughes LE, Nestor PJ, Hodges JR, Rowe JB. Magnetoencephalography of frontotemporal dementia: spatiotemporally localized changes during semantic decisions. *Brain*. 2011:134:2513–2522.

Hughes LE, Rittman T, Regenthal R, Robbins TW, Rowe JB. Improving response inhibition systems in frontotemporal dementia with citalopram. *Brain*. 2015:138:1961–1975.

Hughes LE, Rittman T, Robbins TW, Rowe JB. Reorganization of cortical oscillatory dynamics underlying disinhibition in frontotemporal dementia. *Brain*. 2018:141:2486–2499.

Hung Y, Gaillard SL, Yarmak P, Arsalidou M. Dissociations of cognitive inhibition, response inhibition, and emotional interference: voxelwise ALE meta-analyses of fMRI studies. *Hum Brain Mapp*. 2018:39:4065–4082.

Huster RJ, Enriquez-Geppert S, Lavallee CF, Falkenstein M, Herrmann CS. Electroencephalography of response inhibition tasks: functional networks and cognitive contributions. *Int J Psychophysiol*. 2013:87:217–233.

Ibáñez A. Brain oscillations, inhibition and social inappropriateness in frontotemporal degeneration. *Brain*. 2018:141:e73–e73.

Ibanez A, Manes F. Contextual social cognition and the behavioral variant of frontotemporal dementia. *Neurology*. 2012:78:1354–1362.

Ibanez A, Parra MA, Butler C, for The Latin America and the Caribbean Consortium on Dementia (LAC-CD). The Latin America and the Caribbean consortium on dementia (LAC-CD): from networking to research to implementation science. *J Alzheimers Dis*. 2021a:82:S379–S394.

Ibanez A, Yokoyama JS, Possin KL, Matallana D, Lopera F, Nitrini R, Takada LT, Custodio N, Sosa Ortiz AL, Avila-Funes JA, et al. The multi-partner consortium to expand dementia research in Latin America (ReDLat): driving multicentric research and implementation science. *Front Neurol*. 2021b:12:631722.

Irish M, Piguet O, Hodges JR, Hornberger M. Common and unique gray matter correlates of episodic memory dysfunction in frontotemporal dementia and Alzheimer's disease. *Hum Brain Mapp*. 2014:35:1422–1435.

Jabbi M, Bastiaansen J, Keysers C. A common anterior insula representation of disgust observation, experience and imagination shows divergent functional connectivity pathways. *PLoS One*. 2008:3:e2939.

Jack CR, Petersen RC, Xu YC, Waring SC, O'Brien PC, Tangalos EG, Smith GE, Ivnik RJ, Kokmen E. Medial temporal atrophy on MRI in normal aging and very mild Alzheimer's disease. *Neurology*. 1997:49:786–794.

Jacobs HI, Hopkins DA, Mayrhofer HC, Bruner E, van Leeuwen FW, Raaijmakers W, Schmahmann JD. The cerebellum in Alzheimer's disease: evaluating its role in cognitive decline. *Brain*. 2018:141:37–47.

Kamarajan C, Porjesz B, Jones KA, Choi K, Chorlian DB, Padmanabhapillai A, Rangaswamy M, Stimus AT, Begleiter H. The role of brain oscillations as functional correlates of cognitive systems: a study of frontal inhibitory control in alcoholism. *Int J Psychophysiol*. 2004:51:155–180.

Kanske P, Böckler A, Trautwein F-M, Parianen Lesemann FH, Singer T. Are strong empathizers better mentalizers? Evidence for independence and interaction between the routes of social cognition. *Soc Cogn Affect Neurosci*. 2016:11:1383–1392.

Karch S, Jäger L, Karamatskos E, Graz C, Stammel A, Flatz W, Lutz J, Holtschmidt-Täschner B, Genius J, Leicht G. Influence of trait anxiety on inhibitory control in alcohol-dependent patients: simultaneous acquisition of ERPs and BOLD responses. *J Psychiatr Res*. 2008:42:734–745.

Kaup B, Zwaan RA. Effects of negation and situational presence on the accessibility of text information. *J Exp Psychol Learn Mem Cogn*. 2003:29:439–446.

Kaup B, Yaxley RH, Madden CJ, Zwaan RA, Lüdtke J. Experiential simulations of negated text information. *Q J Exp Psychol*. 2007:60:976–990.

Kiefer M, Sim E-J, Herrnberger B, Grothe J, Hoenig K. The sound of concepts: four markers for a link between auditory and conceptual brain systems. *J Neurosci*. 2008:28:12224–12230.

Kim Y-H, Kim J, Lee J-H. Iterative approach of dual regression with a sparse prior enhances the performance of independent component analysis for group functional magnetic resonance imaging (fMRI) data. *NeuroImage*. 2012:63:1864–1889.

Kolev V, Beste C, Falkenstein M, Yordanova J. Error-related oscillations: effects of aging on neural systems for behavioral monitoring. *J Psychophysiol*. 2009:23:216–223.

Kramer JH, Jurik J, Sharon JS, Rankin KP, Rosen HJ, Johnson JK, Miller BL. Distinctive neuropsychological patterns in frontotemporal dementia, semantic dementia, and Alzheimer disease. *Cogn Behav Neurol*. 2003:16:211–218.

Kuperberg GR, McGuire PK, Bullmore ET, Brammer MJ, Rabe-Hesketh S, Wright IC, Lythgoe DJ, Williams SC, David AS. Common and distinct neural substrates for pragmatic, semantic, and syntactic processing of spoken sentences: an fMRI study. *J Cogn Neurosci*. 2000:12:321–341.

La Joie R, Perrotin A, Barre L, Hommet C, Mezenge F, Ibazizene M, Camus V, Abbas A, Landeau B, Guilloteau DJ, et al. Region-specific hierarchy between atrophy, hypometabolism, and β-amyloid (Aβ) load in Alzheimer's disease dementia. *J Neurosci*. 2012:32:16265–16273.

Lagarde J, Valabrègue R, Corvol J-C, Pineau F, Le Ber I, Vidailhet M, Dubois B, Levy R. Are frontal cognitive and atrophy patterns different in PSP and bvFTD? A comparative neuropsychological and VBM study. *PLoS One*. 2013:8:e80353.

Langenecker SA, Nielson KA, Rao SM. fMRI of healthy older adults during Stroop interference. *NeuroImage*. 2004:21:192–200.

Legaz A, Abrevaya S, Dottori M, Campo CG, Birba A, Caro MM, Aguirre J, Slachevsky A, Aranguiz R, Serrano C, et al. Multimodal mechanisms of human socially reinforced learning across neurodegenerative diseases. *Brain*. 2021. https://doi.org/10.1093/brain/awab345.

Lieberman MD, Cunningham WA. Type I and type II error concerns in fMRI research: re-balancing the scale. *Soc Cogn Affect Neurosci*. 2009:4:423–428.

Liu W, Miller BL, Kramer JH, Rankin K, Wyss-Coray C, Gearhart R, Phengrasamy L, Weiner M, Rosen HJ. Behavioral disorders in the frontal and temporal variants of frontotemporal dementia. *Neurology*. 2004:62:742–748.

Liu B, Wang H, Beltrán D, Gu B, Liang T, Wang X, de Vega M. The generalizability of inhibition-related processes in the comprehension of linguistic negation ERP evidence from the mandarin language. *Language, Cognition and Neuroscience*. 2020:35:7, 885–895. https://doi.org/10.1080/23273798.2019.1662460.

Liu B, Gu B, Beltrán D, Wang H, de Vega M. Presetting an inhibitory state modifies the neural processing of negated action sentences. An ERP study. *Brain Cogn*. 2020:143:105598.

Mannarelli D, Pauletti C, Petritis A, Delle Chiaie R, Currà A, Trompetto C, Fattapposta F. Effects of cerebellar tDCS on inhibitory control: evidence from a go/NoGo task. *Cerebellum*. 2020:19:788–798.

Matías-Guiu JA, Cabrera-Martín MN, Valles-Salgado M, Rognoni T, Galán L, Moreno-Ramos T, Carreras JL, Matías-Guiu J.

Inhibition impairment in frontotemporal dementia, amyotrophic lateral sclerosis, and Alzheimer's disease: clinical assessment and metabolic correlates. *Brain Imaging Behav*. 2019:13:651–659.

McKhann G, Drachman D, Folstein M, Katzman R, Price D, Stadlan EM. Clinical diagnosis of Alzheimer's disease: report of the NINCDS-ADRDA work group under the auspices of Department of Health and Human Services Task Force on Alzheimer's disease. *Neurology*. 1984:34:939–944.

McKhann GM, Knopman DS, Chertkow H, Hyman BT, Jack CR Jr, Kawas CH, Klunk WE, Koroshetz WJ, Manly JJ, Mayeux R, et al. The diagnosis of dementia due to Alzheimer's disease: recommendations from the National Institute on Aging-Alzheimer's Association workgroups on diagnostic guidelines for Alzheimer's disease. *Alzheimers Dement*. 2011:7:263–269.

McMurtray A, Chen A, Shapira J, Chow T, Mishkin F, Miller B, Mendez M. Variations in regional SPECT hypoperfusion and clinical features in frontotemporal dementia. *Neurology*. 2006:66:517–522.

Melloni M, Sedeno L, Hesse E, García-Cordero I, Mikulan E, Plastino A, Marcotti A, Lopez JD, Bustamante C, Lopera F, et al. Cortical dynamics and subcortical signatures of motor-language coupling in Parkinson's disease. *Sci Rep*. 2015:5:11899.

Melloni M, Billeke P, Baez S, Hesse E, De la Fuente L, Forno G, Birba A, García-Cordero I, Serrano C, Plastino A. Your perspective and my benefit: multiple lesion models of self-other integration strategies during social bargaining. *Brain*. 2016:139:1–19.

Mendez MF, Shapira JS. Loss of emotional insight in behavioral variant frontotemporal dementia or "frontal anosodiaphoria". *Conscious Cogn*. 2011:20:1690–1696.

Miestamo M. Negation–an overview of typological research. *Lang Linguist Compass*. 2007:1:552–570.

Mišić B, Sporns O. From regions to connections and networks: new bridges between brain and behavior. *Curr Opin Neurobiol*. 2016:40:1–7.

Moguilner S, García AM, Mikulan E, Hesse E, García-Cordero I, Melloni M, Cervetto S, Serrano C, Herrera E, Reyes P. Weighted symbolic dependence metric (wSDM) for fMRI resting-state connectivity: a multicentric validation for frontotemporal dementia. *Sci Rep*. 2018:8:1–15.

Moguilner S, Birba A, Fino D, Isoardi R, Huetagoyena C, Otoya R, Tirapu V, Cremaschi F, Sedeño L, Ibáñez A, et al. Multimodal neurocognitive markers of frontal lobe epilepsy: insights from ecological text processing. *NeuroImage*. 2021:235:117998.

Moretti DV, Benussi L, Fostinelli S, Ciani M, Binetti G, Ghidoni R. Progranulin mutations affects brain oscillatory activity in frontotemporal dementia. *Front Aging Neurosci*. 2016:8:35.

Nasreddine ZS, Phillips NA, Bedirian V, Charbonneau S, Whitehead V, Collin I, Cummings JL, Chertkow H. The Montreal cognitive assessment, MoCA: a brief screening tool for mild cognitive impairment. *J Am Geriatr Soc*. 2005:53:695–699.

Nasseroleslami B, Dukic S, Broderick M, Mohr K, Schuster C, Gavin B, McLaughlin R, Heverin M, Vajda A, Iyer PM. Characteristic increases in EEG connectivity correlate with changes of structural MRI in amyotrophic lateral sclerosis. *Cereb Cortex*. 2019:29:27–41.

Neary D, Snowden JS, Gustafson L, Passant U, Stuss D, Black S, Freedman M, Kertesz A, Robert PH, Albert M, et al. Frontotemporal lobar degeneration: a consensus on clinical diagnostic criteria. *Neurology*. 1998:51:1546–1554.

Nestor PJ, Fryer TD, Hodges JR. Declarative memory impairments in Alzheimer's disease and semantic dementia. *NeuroImage*. 2006:30:1010–1020.

Nichols TE, Das S, Eickhoff SB, Evans AC, Glatard T, Hanke M, Kriegeskorte N, Milham MP, Poldrack RA, Poline J-B. Best practices in data analysis and sharing in neuroimaging using MRI. *Nat Neurosci*. 2017:20:299.

Nigbur R, Ivanova G, Stürmer B. Theta power as a marker for cognitive interference. *Clin Neurophysiol*. 2011:122:2185–2194.

O'Callaghan C, Bertoux M, Irish M, Shine JM, Wong S, Spiliopoulos L, Hodges JR, Hornberger M. Fair play: social norm compliance failures in behavioural variant frontotemporal dementia. *Brain*. 2016:139:204–216.

O'Callaghan C, Naismith SL, Hodges JR, Lewis SJ, Hornberger M. Fronto-striatal atrophy correlates of inhibitory dysfunction in Parkinson's disease versus behavioural variant frontotemporal dementia. *Cortex*. 2013:49:1833–1843.

O'Connell RG, Dockree PM, Bellgrove MA, Turin A, Ward S, Foxe JJ, Robertson IH. Two types of action error: electrophysiological evidence for separable inhibitory and sustained attention neural mechanisms producing error on go/no-go tasks. *J Cogn Neurosci*. 2009:21:93–104.

Oldfield RC. The assessment and analysis of handedness: the Edinburgh inventory. *Neuropsychologia*. 1971:9:97–113.

Oostenveld R, Fries P, Maris E, Schoffelen J-M. FieldTrip: open source software for advanced analysis of MEG, EEG, and invasive electrophysiological data. *Comput Intell Neurosci*. 2011:2011:156869.

Ossenkoppele R, Pijnenburg YA, Perry DC, Cohn-Sheehy BI, Scheltens NM, Vogel JW, Kramer JH, van der Vlies AE, Joie RL, Rosen HJ, et al. The behavioural/dysexecutive variant of Alzheimer's disease: clinical, neuroimaging and pathological features. *Brain*. 2015:138:2732–2749.

Pandey AK, Kamarajan C, Manz N, Chorlian DB, Stimus A, Porjesz B. Delta, theta, and alpha event-related oscillations in alcoholics during go/NoGo task: neurocognitive deficits in execution, inhibition, and attention processing. *Prog Neuro-Psychopharmacol Biol Psychiatry*. 2016:65:158–171.

Papeo L, Hochmann J-R, Battelli L. The default computation of negated meanings. *J Cogn Neurosci*. 2016:28:1980–1986.

Pasquini L, Nana AL, Toller G, Brown JA, Deng J, Staffaroni A, Kim E-J, Hwang J-HL, Li L, Park Y. Salience network atrophy links neuron type-specific pathobiology to loss of empathy in frontotemporal dementia. *Cereb Cortex*. 2020:30:5387–5399.

Phan KL, Fitzgerald DA, Nathan PJ, Moore GJ, Uhde TW, Tancer ME. Neural substrates for voluntary suppression of negative affect: a functional magnetic resonance imaging study. *Biol Psychiatry*. 2005:57:210–219.

Piguet O, Hornberger M, Mioshi E, Hodges JR. Behavioural-variant frontotemporal dementia: diagnosis, clinical staging, and management. *Lancet Neurol*. 2011:10:162–172.

Poldrack RA, Baker CI, Durnez J, Gorgolewski KJ, Matthews PM, Munafò MR, Nichols TE, Poline J-B, Vul E, Yarkoni T. Scanning the horizon: towards transparent and reproducible neuroimaging research. *Nat Rev Neurosci*. 2017:18:115.

Polich J. Updating P300: an integrative theory of P3a and P3b. *Clin Neurophysiol*. 2007:118:2128–2148.

Premi E, Cauda F, Gasparotti R, Diano M, Archetti S, Padovani A, Borroni B. Multimodal FMRI resting-state functional connectivity in granulin mutations: the case of fronto-parietal dementia. *PLoS One*. 2014:9:e106500.

Pulvermüller F. Semantic embodiment, disembodiment or misembodiment? In search of meaning in modules and neuron circuits. *Brain Lang*. 2013:127:86–103.

Pulvermüller F. Neural reuse of action perception circuits for language, concepts and communication. *Prog Neurobiol*. 2018:160:1–44.

Ranasinghe KG, Rankin KP, Pressman PS, Perry DC, Lobach IV, Seeley WW, Coppola G, Karydas AM, Grinberg LT, Shany-Ur T, et al.

Distinct subtypes of behavioral variant frontotemporal dementia based on patterns of network degeneration. *JAMA Neurol*. 2016:73: 1078–1088.

Rascovsky K, Hodges JR, Knopman D, Mendez MF, Kramer JH, Neuhaus J, Van Swieten JC, Seelaar H, Dopper EG, Onyike CU. Sensitivity of revised diagnostic criteria for the behavioural variant of frontotemporal dementia. *Brain*. 2011:134: 2456–2477.

Redick TS, Calvo A, Gay CE, Engle RW. Working memory capacity and go/no-go task performance: selective effects of updating, maintenance, and inhibition. *J Exp Psychol Learn Mem Cogn*. 2011:37: 308–324.

Salamone PC, Esteves S, Sinay VJ, García-Cordero I, Abrevaya S, Couto B, Adolfi F, Martorell M, Petroni A, Yoris A, et al. Altered neural signatures of interoception in multiple sclerosis. *Hum Brain Mapp*. 2018:39:4743–4754.

Salamone PC, Legaz A, Sedeño L, Moguilner S, Fraile-Vazquez M, Campo CG, Fittipaldi S, Yoris A, Miranda M, Birba A. Interoception primes emotional processing: multimodal evidence from neurodegeneration. *J Neurosci*. 2021:41:4276–4292.

Sami S, Williams N, Hughes LE, Cope TE, Rittman T, Coyle-Gilchrist IT, Henson RN, Rowe JB. Neurophysiological signatures of Alzheimer's disease and frontotemporal lobar degeneration: pathology versus phenotype. *Brain*. 2018:141: 2500–2510.

Santamaría-García H, Baez S, Reyes P, Santamaría-García JA, Santacruz-Escudero JM, Matallana D, Arévalo A, Sigman M, García AM, Ibáñez A. A lesion model of envy and schadenfreude: legal, deservingness and moral dimensions as revealed by neurodegeneration. *Brain*. 2017:140:3357–3377.

Santamaría-García H, Ibáñez A, Montaño S, García AM, Patiño-Saenz M, Idarraga C, Pino M, Baez S. Out of context, beyond the face: neuroanatomical pathways of emotional face-body language integration in adolescent offenders. *Front Behav Neurosci*. 2019:13:34.

Santillo AF, Lundblad K, Nilsson M, Landqvist Waldö M, Van Westen D, Lätt J, Blennow Nordström E, Vestberg S, Lindberg O, Nilsson C. Grey and white matter clinico-anatomical correlates of disinhibition in neurodegenerative disease. *PLoS One*. 2016:11: e0164122.

Scheltens NM, van der Weijden K, Adriaanse SM, van Assema D, Oomen PP, Krudop WA, Lammertsma AA, Barkhof F, Koene T, Teunissen CE. Hypometabolism of the posterior cingulate cortex is not restricted to Alzheimer's disease. *NeuroImage Clin*. 2018:19: 625–632.

Schmiedt-Fehr C, Basar-Eroglu C. Event-related delta and theta brain oscillations reflect age-related changes in both a general and a specific neuronal inhibitory mechanism. *Clin Neurophysiol*. 2011:122:1156–1167.

Sedeno L, Piguet O, Abrevaya S, Desmaras H, García-Cordero I, Baez S, Alethia de la Fuente L, Reyes P, Tu S, Moguilner S, et al. Tackling variability: a multicenter study to provide a gold-standard network approach for frontotemporal dementia. *Hum Brain Mapp*. 2017:38:3804–3822.

Sollberger M, Stanley CM, Wilson SM, Gyurak A, Beckman V, Growdon M, Jang J, Weiner MW, Miller BL, Rankin KP. Neural basis of interpersonal traits in neurodegenerative diseases. *Neuropsychologia*. 2009:47:2812–2827.

Stopford CL, Thompson JC, Neary D, Richardson AM, Snowden JS. Working memory, attention, and executive function in Alzheimer's disease and frontotemporal dementia. *Cortex*. 2012:48:429–446.

Tettamanti M, Manenti R, Della Rosa PA, Falini A, Perani D, Cappa SF, Moro A. Negation in the brain: modulating action representations. *NeuroImage*. 2008:43:358–367.

Tomasino B, Weiss PH, Fink GR. To move or not to move: imperatives modulate action-related verb processing in the motor system. *Neuroscience*. 2010:169:246–258.

Tzourio-Mazoyer N, Landeau B, Papathanassiou D, Crivello F, Etard O, Delcroix N, Mazoyer B, Joliot M. Automated anatomical labeling of activations in SPM using a macroscopic anatomical parcellation of the MNI MRI single-subject brain. *NeuroImage*. 2002:15:273–289.

Uludağ K, Roebroeck A. General overview on the merits of multimodal neuroimaging data fusion. *NeuroImage*. 2014:102: 3–10.

van Loenhoud AC, Wink AM, Groot C, Verfaillie SC, Twisk J, Barkhof F, van Berckel B, Scheltens P, van der Flier WM, Ossenkoppele R. A neuroimaging approach to capture cognitive reserve: application to Alzheimer's disease. *Hum Brain Mapp*. 2017:38: 4703–4715.

Vilas MG, Santilli M, Mikulan E, Adolfi F, Caro MM, Manes F, Herrera E, Sedeño L, Ibáñez A, García AM. Reading Shakespearean tropes in a foreign tongue: age of L2 acquisition modulates neural responses to functional shifts. *Neuropsychologia*. 2019:124: 79–86.

Vitale F, Monti I, Padrón I, Avenanti A, de Vega M. The neural inhibition network is causally involved in the disembodiment effect of linguistic negation. *Cortex*. 2022:147:72–82.

Whitwell JL, Przybelski SA, Weigand SD, Ivnik RJ, Vemuri P, Gunter JL, Senjem ML, Shiung MM, Boeve BF, Knopman DS. Distinct anatomical subtypes of the behavioural variant of frontotemporal dementia: a cluster analysis study. *Brain*. 2009:132:2932–2946.

Willems RM, Hagoort P, Casasanto D. Body-specific representations of action verbs: neural evidence from right-and left-handers. *Psychol Sci*. 2010:21:67–74.

Wingfield A, Grossman M. Language and the aging brain: patterns of neural compensation revealed by functional brain imaging. *J Neurophysiol*. 2006:96:2830–2839.

Wlotko EW, Federmeier KD, Kutas M. To predict or not to predict: age-related differences in the use of sentential context. *Psychol Aging*. 2012:27:975–988.

Woo C-W, Krishnan A, Wager TD. Cluster-extent based thresholding in fMRI analyses: pitfalls and recommendations. *NeuroImage*. 2014:91:412–419.

Yaple ZA, Stevens WD, Arsalidou M. Meta-analyses of the n-back working memory task: fMRI evidence of age-related changes in prefrontal cortex involvement across the adult lifespan. *NeuroImage*. 2019:196:16–31.

Yener G, Güntekin B, Başar E. Event-related delta oscillatory responses of Alzheimer patients. *Eur J Neurol*. 2008:15:540–547.

Yoris A, Abrevaya S, Esteves S, Salamone P, Lori N, Martorell M, Legaz A, Alifano F, Petroni A, Sánchez R, et al. Multilevel convergence of interoceptive impairments in hypertension: new evidence of disrupted body–brain interactions. *Hum Brain Mapp*. 2018:39: 1563–1581.

Young L, Bechara A, Tranel D, Damasio H, Hauser M, Damasio A. Damage to ventromedial prefrontal cortex impairs judgment of harmful intent. *Neuron*. 2010:65:845–851.

Yu M, Gouw AA, Hillebrand A, Tijms BM, Stam CJ, van Straaten EC, Pijnenburg YA. Different functional connectivity and network topology in behavioral variant of frontotemporal dementia and Alzheimer's disease: an EEG study. *Neurobiol Aging*. 2016:42: 150–162.

Yu-Feng Z, Yong H, Chao-Zhe Z, Qing-Jiu C, Man-Qiu S, Meng L, Li-Xia T, Tian-Zi J, Yu-Feng W. Altered baseline brain activity in children with ADHD revealed by resting-state functional MRI. *Brain and Development*. 2007:29:83–91.

Zamboni G, Huey E, Krueger F, Nichelli PF, Grafman J. Apathy and disinhibition in frontotemporal dementia: insights into their neural correlates. *Neurology*. 2008:71:736–742.

Zheng D, Oka T, Bokura H, Yamaguchi S. The key locus of common response inhibition network for no-go and stop signals. *J Cogn Neurosci*. 2008:20:1434–1442.

Zheng W, Liu X, Song H, Li K, Wang Z. Altered functional connectivity of cognitive-related cerebellar subregions in Alzheimer's disease. *Front Aging Neurosci*. 2017:9:143.